Niobocene Silyl Hydride Complexes with Nonclassical Interligand Hypervalent Interactions

Georgii I. Nikonov,*[a] Lyudmila G. Kuzmina,[b] Sergei F. Vyboishchikov,[a] Dmitry A. Lemenovskii,[a] and Judith A. K. Howard[c]

Abstract: Reaction of $[Cp_2NbBH_4]$ with tertiary silanes $HSiR_3$ ($R_3 = (OEt)_3$, Me_2Ph, Me_2Cl) in the presence of an amine affords monosilyl complexes $[Cp_2NbH_2SiR_3]$ ($R_3 = (OEt)_3$ (**1**), Me_2Ph (**2**), Me_2Cl (**3**)). Complex **3** was obtained as a mixture of two isomers, with the silyl ligand in the lateral (**3b**) and central (**3a**) positions. The more sterically strained isomer **3b** was obtained in a slightly greater amount than **3a**, signifying the presence of an additional stabilizing electronic factor. Complex **3b** was shown to be a thermodynamic product of the reaction. Thermal reaction of $[Cp_2NbH_3]$ with $HSiMe_2Cl$ at 50 °C gives initially a mixture of **3a** and **3b**, but under more severe conditions (at 90 °C) unprecedented dihydrogen elimination occurs to yield the bis(silyl) complex $[Cp_2NbH(SiMe_2Cl)_2]$. Complexes $[Cp_2NbH(SiMe_2X)_2]$ (X = Cl (**4**), Ph (**6**)) were obtained by reaction of $[Cp_2NbH(C_2H_3Ph)]$ with the corresponding silanes $HSiMe_2X$. Reduction of complex **4** by $LiAlH_4$ gives a high yield of $[Cp_2NbH(SiMe_2H)_2]$, which reacts with $[Ph_3C]PF_6$ and $Br_2 \cdot$ dioxane to afford bis(silyl) complexes $[Cp_2NbH(SiMe_2F)_2]$ (**8**) and $[Cp_2NbH(SiMe_2X)_2]$ (**9**), respectively. Compounds **3b**, **4**, **6**, **8** and **9** were studied by NMR and IR spectroscopy and X-ray diffraction analysis. The X-ray data for **3b**, **4**, **8** and **9**, together with some reactivity trends, suggest a nonclassical nature of these complexes due to the presence of interligand interaction between the silyl and hydride ligands. The observed trends in structural parameters are different from those predicted for three-center, two-electron (3c–2e) interactions of silanes with transition metals. This new type of nonclassical bonding was rationalized as a hypervalent interaction at the silicon centre due to the overlap of the Nb–H bonding orbital and the Si–Cl antibonding orbital. The main structural trends as well as the occurrence of an Nb–H →Si–Cl* electron density transfer were supported by natural bond orbital (NBO) analysis. The calculation results show stronger interligand interactions in the chlorosilyl complexes than in the corresponding SiH_3 complexes. However, a correlation between the structural and NMR parameters for the niobocene silyl hydrides was not established because of the unfavourable influence of the quadrupolar niobium nucleus.

Keywords: ab initio calculations · hydrido complexes · hypervalent compounds · niobium · silicon

Introduction

Reductive elimination and migratory insertion reactions are fundamental processes important for both industrial and academic chemistry.[1] In spite of the wide application of these reactions, little is yet known about their mechanisms. Both types of reactions are accompanied by metal–ligand bond breaking and ligand–ligand bond formation. Intuitively, it is apparent that there should be some kind of interligand interaction in the intermediate stages of these transformations (Scheme 1). It is also clear that these interactions should be of

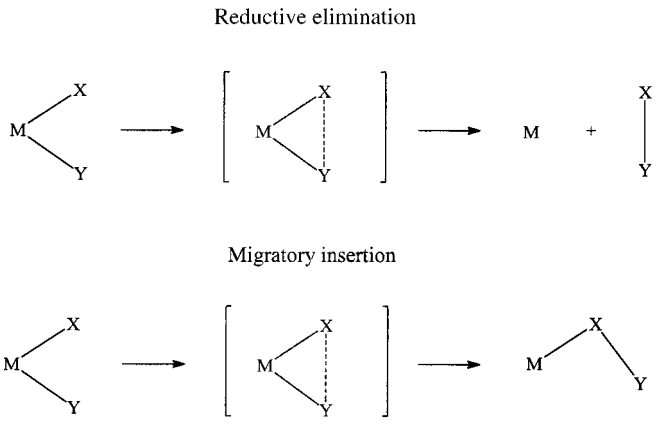

Scheme 1. Examples of interligand interactions in transition metal mediated transformations.

[a] Dr. G. I. Nikonov, Dr. S. F. Vyboishchikov, Prof. Dr. D. A. Lemenovskii
Chemistry Department, Moscow State University
Vorob'evy Gory, 119899 Moscow (Russia)
Fax: (+7) 95-932-88-46
E-mail: nikonov@org.chem.msu.su

[b] Prof. Dr. L. G. Kuzmina
Institute of General and Inorganic Chemistry, RAS
Leninsky Prosp. 31, 117907 Moscow (Russia)

[c] Prof. Dr. J. A. K. Howard
Chemistry Department, University of Durham
South Road, Durham DH1 3LE (UK)

  0947-6539/99/0510-2947 $ 17.50+.50/0

Abstract in Russian: Реакция комплекса $[Cp_2NbBH_4]$ с силанами $HSiR_3$ ($R_3 = (OEt)_3$, Me_2Ph, Me_2Cl) в присутствии триэтиламина приводит к образованию моносилильных комплексов $[Cp_2NbH_2SiR_3]$ ($R_3 = (OEt)_3$ (**1**), Me_2Ph (**2**), Me_2Cl (**3**)). Соединение **3** было получено в виде смеси двух изомеров: с боковым (**3b**) и центральным (**3a**) положением кремниевого лиганда. Стерически более напряженный изомер **3b** образуется с несколько большим выходом, чем **3a**, что свидетельствует о наличии дополнительного стабилизирующего электронного фактора. Оказалось, что комплекс **3b** является термодинамическим продуктом реакции. Нагревание смеси Cp_2NbH_3 и $HSiMe_2Cl$ при 50°C первоначально дает смесь изомеров **3a** and **3b**, но при дальнейшем нагревании до 90°C происходит отщепление молекулы водорода с образованием дисилильного комплекса $[Cp_2NbH(SiMe_2Cl)_2]$. Соединения $[Cp_2NbH(SiMe_2X)_2]$ (X = Cl (**4**), Ph (**6**)) были получены по реакции $[Cp_2NbH(C_2H_3Ph)]$ с соответствующими силанами $HSiMe_2X$. Восстановление **4** под действием $LiAlH_4$ дает высокий выход комплекса $[Cp_2NbH(SiMe_2H)_2]$, который реагирует с $[Ph_3C]PF_6$ и Br_2*диоксан с образованием дисилильных комплексов $[Cp_2NbH(SiMe_2F)_2]$ (**8**) и $[Cp_2NbH(SiMe_2X)_2]$ (**9**), соответственно. Соединения **3b**, **4**, **6**, **8**, **9** были изучены методами ЯМР- и ИК-спектроскопии, а также РСА. Данные РСА для **3b**, **4**, **8** и **9** и их реакционная способность позволяют сделать вывод, что в них присутствует неклассическое межлигандное взаимодействие между кремниевыми и гидридными лигандами. Структурные параметры, наблюдаемые в этих соединениях, отличаются от предсказываемых теорией 3c-2e взаимодействий силанов с переходными металлами. Этот новый тип неклассического связывания был объяснен как гипервалентное взаимодействие при кремниевым центре, благодаря перекрыванию Nb–H связывающей орбитали и Si–Cl антисвязывающей орбитали. Основные тенденции в структурных параметрах, а также наличие переноса электронной плотности Nb–H→Si–Cl*, были также подтверждены с помощью расчётов методом функционала плотности. Наличие прямого связывания Si–H следует из больших значений индексов связи по Вибергу и наблюдаемой "линии связи" по Бейдеру в комплексе **3b** и его модели **11**, а также нашло дальнейшее подтверждение в анализе по методу натуральных орбиталей связи. Результаты расчётов свидетельствуют о более сильном межлигандном взаимодействии в хлорсилильных комплексах по

a nonclassical type and their study would shed a significant light on the nature of reductive elimination, oxidative addition and migratory insertion reactions. Preparation of complexes containing nonclassical interligand interactions is, therefore, an important goal of synthesis.

The fascinating discovery by Kubas and others of σ-complexes[2] made a great contribution to our understanding of oxidative addition and its reverse, reductive elimination. Factors such as the effect of the metal, the influence of charge and the nature of the supporting ligands have been well documented. In contrast, the nature of migratory insertion is less well understood. Probably the only examples of non-classical interligand interactions that model this reaction are the β-agostic M, C, H complexes that model the migration of a hydride onto a coordinated olefin ligand. We have recently reported a new type of nonclassical interaction between two silyl ligands (in the α position relative to the metal) and a hydride.[3] This bonding mode was rationalized in terms of interligand hypervalent interaction (IHI). Later Gountchev and Tilley reported a similar interligand interaction between a β-positioned silicon centre and a hydride ligand.[4]

Here we report structural and reactivity studies on a series of niobocene hydride complexes, substituted by halosilyl ligands SiR_2X (X = F, Cl, Br). The observed trends suggest that these complexes have an interligand hypervalent interaction. Also, IHI between *one* hydride and *one* silyl is reported for the first time. The nature of interligand interactions is further studied by means of quantum chemical calculations for model compounds.

Results and Discussion

Oxidative addition route to the monosilyl derivatives of niobocene: Early transition metal silyl complexes, $L_nM{-}SiR_3$, have recently attracted great interest.[5–9] The substituents R at silicon are usually chemically robust alkyl and aryl groups, and more rarely hydrogen. Early transition metal complexes substituted by functionalized silyl groups are quite rare and have been prepared only very recently.[5c,d] The usual synthetic strategies available to make silyl derivatives involve conventional metathetical procedures,[6, 7a] oxidative addition of silanes[5, 7] and in the case of d^0 complexes σ-bond metathesis reactions.[8] The oxidative addition of a silane Si–H bond is a particularly useful method for the preparation of silyl hydride complexes.[5, 6a, 7] Thus, the thermal reaction of $[Cp_2NbH_3]$ with $HSiMe_2Ph$, believed to proceed through the intermediate $[Cp_2NbH]$, gives $[Cp_2NbH_2SiMe_2Ph]$ in high yield.[7g] Complexes of the type $[(C_5H_4SiMe_3)_2NbH_2SiMe_xPh_{3-x}]$ have been prepared analogously.[7c] Berry et al. showed that oxidative addition of functionalized silanes $HSiR_2X$ (X = Cl, R = Me; $XR_2 = (OMe)_3$) to tantalocenes gave high yields of the corresponding silyl hydride complexes.[5c] In contrast, the reaction of $[Cp_2NbH_3]$ with siloxane $HSiMe_2OSiMe_3$ was not clean and furnished a mixture of products.[7g] Another limitation of this method comes from the low thermal stability of some silyl products. Thus, thermolysis of $[Cp_2NbH_3]$ in the presence of $HSiEt_3$ gave only bis(niobocene)[10] although labelling experiments indicated the intermediate complex-

0947-6539/99/0510-2948 $ 17.50+.50/0 *Chem. Eur. J.* **1999**, *5*, No. 10

ation of a silane to niobocene.[7g] When we attempted to prepare $[Cp_2NbH_2Si(OEt)_3]$ (**1**) by this method, we observed a similar result: heating a solution of $[Cp_2NbH_3]$ and $HSi(OEt)_3$ in toluene afforded a high yield of bis(niobocene).

To achieve the oxidative addition of silanes under milder conditions, we allowed silanes to react with the readily accessible complex $[Cp_2NbBH_4]$ in the presence of NEt_3 [Eq. (1)]. It had been shown previously that addition of an amine to $[Cp_2NbBH_4]$ generated a reactive intermediate that behaved as $[Cp_2NbH]$ and thus was amenable to the oxidative addition reaction.[11] All the complexes in Equation (1) were prepared in high yields and were characterized spectroscopically. Complex **3b** was also studied by X-ray diffraction analysis. Compounds **1** and **2** are yellow and **3** is colourless. These materials are highly air-sensitive.

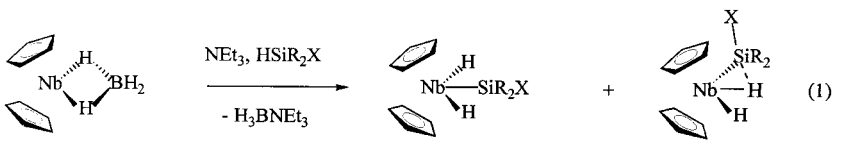

1-3a **3b**

1: R = X = OEt

2: R = Me, X = Ph

3: R = Me, X = Cl

Only the symmetric isomer, with the central position of the silyl group in the bisecting plane of the niobocene moiety, was observed for complexes **1** and **2**. In contrast, addition of $HSiMe_2Cl$ affords two isomers, with the silyl group in the central (**3a**) and lateral (**3b**) positions, in the ratio 1:1.2. In the related tantalocene chemistry oxidative addition of silanes to $[Cp_2TaH]$ gives both isomers, the asymmetric (lateral) one being the kinetic product. Upon heating the asymmetric isomers of $[Cp_2TaH_2SiR_3]$ rearrange intramolecularly into the symmetric ones at a rate that depends on the nature of the substituents R.[5c] We found that heating the mixture of **3a** and **3b** at 70 °C for 3 h did not change the ratio of isomers. The reaction was conducted in a sealed NMR tube in C_6D_6 and was monitored by NMR spectroscopy. Increasing the temperature to 95 °C resulted in decomposition of the monosilyl complexes **3** and appearance of the bis(silyl) complex $[Cp_2NbH(SiMe_2Cl)_2]$ (**4**). This reaction will be discussed in some detail below. Here it is important to note that the ratio of the **3a** and **3b** still unreacted during this process remained unchanged at 1:1.2. We conclude that the asymmetric isomer **3b** is the thermodynamically more stable one; thus it is not a kinetic product of the oxidative addition of silane as was observed in the chemistry of tantalocene. Intuitively, it is apparent that the asymmetric isomer should suffer greater steric strain than the symmetric one due to the closer proximity of the silyl substituent to the cyclopentadienyl rings. The molecular mechanics calculations show that the symmetric isomer **3a** is 6.5 kcal mol^{-1} less strained than **3b**. Therefore, we assume that there should be an additional stabilizing factor in **3b** that must be electronic in nature. We suggest that this arises in the form of an interligand interaction between the silyl and hydride ligands. All the data presented below, including the X-ray structure determination of **3b**, are in accord with this conclusion.

The presence of an electron-withdrawing chlorine substituent at silicon is essential for the interligand interaction and thus for the stabilization of the asymmetric isomer **3b**. Addition of one equivalent of MeLi to the mixture of **3a** and **3b** results in the smooth substitution of Cl for Me and formation of the known compound $[Cp_2NbH_2(SiMe_3)]$ (**5a**).[7a] Only the symmetric isomer **5a** was observed even when the reaction took place in an NMR tube and the spectrum was recorded immediately after mixing the reagents. It seems logical to assume that the asymmetric complex **3b** reacts with MeLi to form the asymmetric complex **5b** initially and that it rearranges rapidly into the symmetric complex **5a** [Eq. (2)].

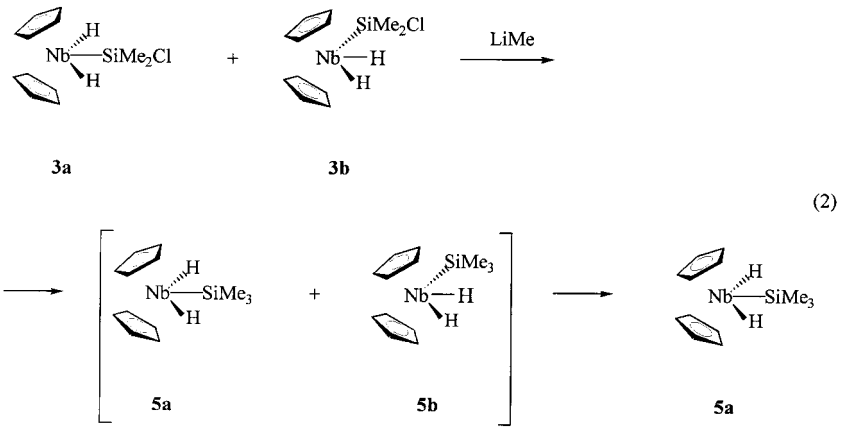

3a **3b**

5a **5b** **5a**

A mixture of **3a** and **3b** can also be conveniently prepared by thermolysis of $[Cp_2NbH_3]$ in the presence of $HSiMe_2Cl$. We failed to separate the isomers **3a** and **3b** by the usual crystallization techniques. Attempted crystallization afforded only microcrystalline materials, which could not be separated manually. Relatively large crystals, suitable for X-ray studies, were composed only of **3b**. All attempts to grow an X-ray quality crystal of **3a** failed.

Oxidative addition route to the bis(silyl) derivatives of niobocene: Bis(silyl) derivatives of tantalocenes were first prepared by Berry et al. by the oxidative addition of silanes to the transient $[Cp_2TaCH_3]$ generated in situ from the precursor $[Cp_2Ta(L)CH_3]$.[5c] Bercaw et al.[12] showed that the niobocene olefin hydride complex $[Cp_2Nb(L)H]$ ($L = C_2H_4$, styrene and so on) could serve as a synthon for the reactive alkyl derivatives $[Cp_2Nb{-}Alk]$ according to the equilibrium shown in Equation (3).

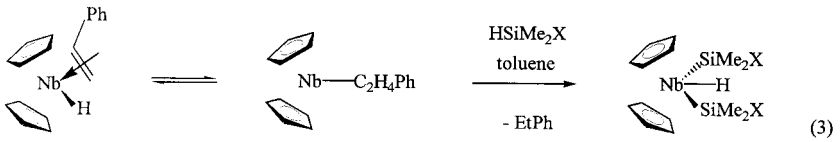

(3)

4 X = Cl

6 X = Ph

Thus, thermolysis of $[Cp_2Nb(styrene)H]$ in the presence of $HSnMe_3$ afforded the bis(stannyl) derivative $[Cp_2NbH(SnMe_3)_2]$, the mechanism being analogous to that proposed for $[Cp_2TaH(SiR_3)_2]$.[13] We used this strategy to prepare the first bis(silyl) hydride derivatives of niobocene [Eq. (3)].[3] Complexes **4** and **6** were isolated as crystalline materials in high yields. Complex **6** is extremely air-sensitive both in solution and as a solid, as are the monosilyl derivatives **1**–**3**. In contrast, the crystalline form of **4** is stable for hours even when exposed to air. Surprisingly, its solutions are also quite stable in air; fast decantation of a benzene solution of **4** in air from one NMR tube into another resulted in only a 20% decrease in the ^1H NMR signal intensity. All the other silyl derivatives considered above decompose completely under these conditions. Another surprising example of the chemical stability of **4** was its behaviour towards chlorinated solvents. It is well known that metallocene hydrides react rapidly with halogenated organic compounds to form the corresponding halogen–hydrogen exchange products.[14] We found that **4** is indefinitely stable in CH_2Cl_2 and $CHCl_3$. It also shows no sign of decomposition when heated under reflux for some hours in toluene. From the remarkable chemical inertness of **4** we conclude that there is additional stabilization in this compound that probably arises from an interaction between the silyl and hydride ligands. Since the position of these ligands in **4** and in **3b** relative to the other groups is analogous, this factor should also operate for the monosilyl complex **3b**, thus explaining its unusual thermal stability. To test this hypothesis, we studied the reaction of a fivefold excess of CH_2Cl_2 with a mixture of **3a** and **3b**, which we monitored by NMR spectroscopy. Both complexes do react with CH_2Cl_2, as was evident from a decrease in their Cp signal relative to the internal standard ($SiMe_4$), the products being $[Cp_2NbCl_2]$, CH_3Cl and $HClSiMe_2$. However, the ratio of the unreacted **3a** and **3b** after one day of reaction was 1:5, in contrast to the ratio of 1:1.2 in the thermal preparations. This observation leads to two conclusions. First, the rearrangement of **3b** into **3a** is relatively slow at room temperature. Second, **3b** is more inert than **3a**. We think that the reactivity of **3b** towards CH_2Cl_2 is due to the lateral hydride ligand that is not involved in the nonclassical interaction with the silyl ligand (vide infra).

As stated above, the thermolysis of a mixture of **3a** and **3b** at 95 °C results in formation of **4**. From this reaction in a sealed NMR tube, the yield of **4** was about 50% (by integration). The nature of the other products of this reaction is as yet unknown. Furthermore, heating **3** in the presence of $HClSiMe_2$ gave an almost quantitative yield of **4**, which is further evidence in favour of an equilibrium between **3a** and **3b** at high temperatures. Thus, the most convenient route to **4** is the thermolysis of toluene solutions of $[Cp_2NbH_3]$ and an excess of $HClSiMe_2$. Heating this mixture at temperatures about 50 °C gives a mixture of complexes **3a** and **3b** exclusively. A further increase in the temperature to 95 °C affords **4** as the sole product. The key step in the possible mechanism of this reaction (Scheme 2) is the elimination of dihydrogen from **3b** to give the 16e complex $[Cp_2NbSiClMe_2]$. The symmetrical complex **3a** is in equilibrium with **3b** and can also release free $HSiClMe_2$. In the absence of added silane this decomposition reaction is the source of $HSiClMe_2$ which further combines with $[Cp_2NbSiClMe_2]$ to give **4** eventually. Dihydrogen elimina-

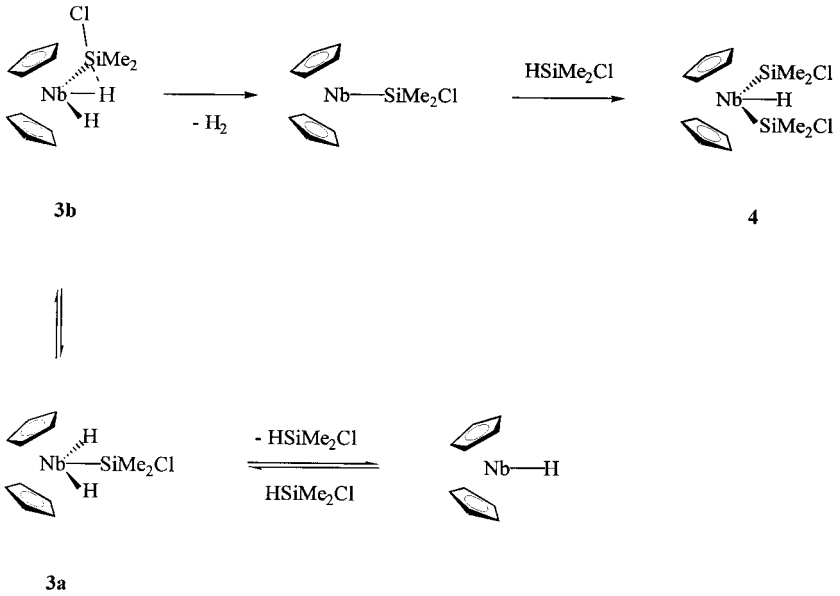

Scheme 2. Possible mechanism of conversion of $[Cp_2NbH_2(SiMe_2Cl)]$ (**3**) into $[Cp_2NbH(SiMe_2Cl)_2]$ (**4**).

0947-6539/99/0510-2950 $ 17.50+.50/0 *Chem. Eur. J.* **1999**, *5*, No. 10

tion, analogous to that from **3b**, has been observed previously in the thermal decomposition of the tin complex $[Cp_2NbH_2SnMe_3]$, affording the bis(stannyl) complex $[Cp_2NbH(SnMe_3)_2]$.[13] In contrast, the mono(silyl) niobocene complexes $[Cp_2NbH_2SiR_3]$ (R = Alk, Ar) displayed only silane elimination.[7a,g]

Preparation of bis(silyl) complexes $[Cp_2NbH(SiMe_2X)_2]$ (X = F, Br) by electrophilic cleavage of the Si–H bond: Reaction of the Si–H bonds of silanes with electrophiles E–X is a well-known method of generating Si–X bonds. We used this approach in the synthesis of bis(halosilyl) complexes $[Cp_2NbH(SiMe_2X)_2]$ (X = F, Br). The precursor complex $[Cp_2NbH(SiMe_2H)_2]$ (**7**) can be prepared easily by reduction of the readily available complex **4** according to Equation (4). Complex **7** was reliably characterized by its NMR and IR spectra and further chemical transformations. In the

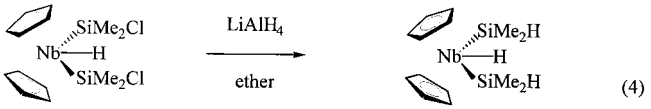

(4)

4 **7**

^{1}H NMR spectrum of **7** the resonances due to the cyclopentadienyl protons and hydride ligand appear as singlets at $\delta = 4.36$ and -3.82, respectively. The methyl groups give rise to a doublet at $\delta = 0.49$ ($J = 3.5$ Hz) due to the coupling with the Si–H proton. The latter exhibits a septet at $\delta = 4.98$ ($J = 3.5$ Hz) in a region typical of Si–H resonances. The band at 1987 cm^{-1} in the IR spectrum also confirms the presence of an Si–H bond.

The direct fluorination of the Si–H bond with fluorine is hardly feasible, but the use of reagents based on the trityl cation $[Ph_3C][EF_n]$ (E = B, $n = 4$; E = P, $n = 6$) provides a good alternative. Although there was some indication in the literature that the use of the hexafluorophosphate counterion may not result in Si–F bond formation,[15] the reaction between **7** and $[Ph_3C][PF_6]$ gave a reasonably high yield of the fluorinated complex $[Cp_2NbH(SiMe_2F)_2]$ (**8**) [Eq. (5)],

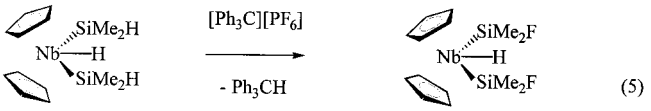

(5)

7 **8**

which was isolated as pale crystals after recrystallization from hexanes. Its thermal stability and sensitivity to air are analogous to those of the related complex **4**. The NMR features of **8** are also similar to those of **4**, the main difference being that the methyl group resonance of **8** appears as a doublet at $\delta = 0.52$ ($^3J_{F,H} = 7.5$ Hz) due to the coupling with the ^{19}F atom. The ^{19}F NMR signal was also observed as a singlet at $\delta = -125.6$. The molecular structure of this compound was reliably established by X-ray diffraction (vide infra).

Reaction of **7** with $Br_2 \cdot$dioxane in ether results in fast precipitation of a light beige material and formation of a light yellow solution. Filtration and removal of the solvent result in large, pale pink crystals of the brominated product $[Cp_2NbH(SiMe_2Br)_2]$ (**9**) [Eq. (6)]. The formation of this product was confirmed by spectroscopic and X-ray diffraction

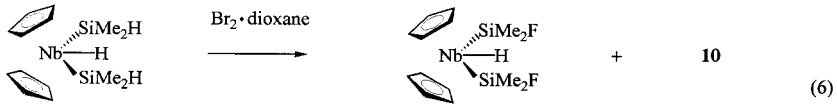

(6)

7 **9**

methods. The precipitate obtained was almost completely insoluble in all available organic solvents and its structure remains unknown. We tentatively formulate this material as the salt $[Cp_2Nb(SiMe_2Br)(SiMe_2H)]Br$ (**10**). A somewhat similar salt, $[Cp_2TaMe_2]Br$, was prepared by Schrock and Sharp by the action of bromine on $[Cp_2TaMe_3]$;[16] it also was insoluble in organic solvents. Surprisingly, when reaction (6) was carried out in the presence of an amine to consume the HBr released, initially there were no niobocene products that were soluble in diethyl ether. However, when the white voluminous precipitate obtained was kept under the mother liquor, a soluble product was formed. It was identified by its ^{1}H NMR spectrum to be pure $[Cp_2NbH_3]$![17] Heating **10** in THF at 65 °C for 2 h resulted in a brown crystalline material, sparingly soluble in THF and insoluble in nonpolar solvents; its ^{1}H NMR ($[D_8]$THF) spectrum showed a weak singlet at $\delta = 5.55$, possibly attributable to the cyclopentadienyl protons. The nature of these materials and the routes by which they are formed are unclear at present.

Complex **9** is among the first transition metal silyl complexes reported to have an Si–Br bond. The mechanism of formation of this complex is not straightforward and will be the subject of further studies. One possibility is that the Si–Br bond emerges as a result of a direct attack by Br_2 on the Si–H bonds. This reaction is analogous to the interaction of silanes R_3SiH with bromine. However, we favour an alternative mechanism involving an electrophilic attack of a bromonium ion on the more electron-rich Nb–H bond to give the cation $[Cp_2Nb(SiMe_2H)(SiMe_2H)]^+$ initially. Attack of the bromide anion on the silicon centre followed by hydrogen migration from silicon to metal would yield the monohalogenated complex $[Cp_2Nb(SiMe_2H)(SiMe_2Br)H]$. Repetition of this sequence of reactions would eventually give complex **9**.

X-ray diffraction studies: The molecular structures of four bis- and one mono(silyl) niobocene compounds were determined. Coupled with the data on other transition metal silyl complexes, these results provide strong evidence in favour of nonclassical interligand interactions in complexes **3b**, **4**, **8** and **9**. The bromine complex **9** is the first reported example of a transition metal complex substituted by a bromosilyl ligand

that has been characterized by X-ray diffraction. The molecular structures of complexes **3b**, **4**, **6**, **8** and **9** are shown in Figures 1–5. Some important bond lengths and angles are summarized in Tables 1 and 2, where relevant literature data are also given for comparison. Examination of the variation of the Nb–Si bond lengths across the series of bis(silyl) complexes $[Cp_2M(SiMe_2X)_2H]$ (M = Nb, Ta) reveals a considerable decrease in this distance on changing the groups X = Ph, H for more electronegative halogen substituents. Two factors are responsible for this shortening. One is the well-known "rehybridization" effect, also

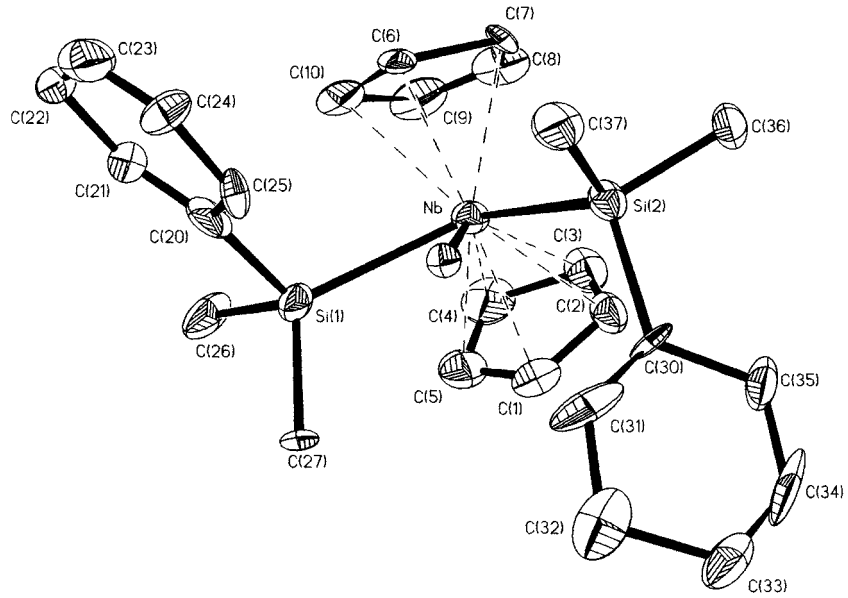

Figure 3. Molecular structure of **6**.

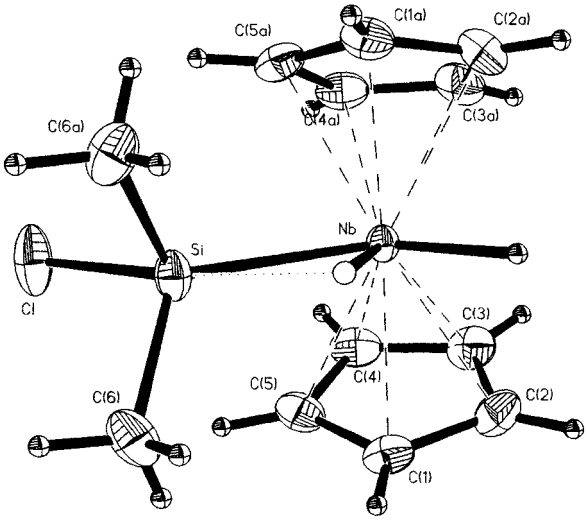

Figure 1. Molecular structure of **3b**.

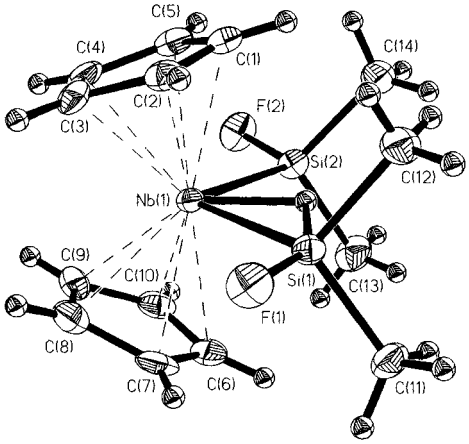

Figure 4. Molecular structure of **8**.

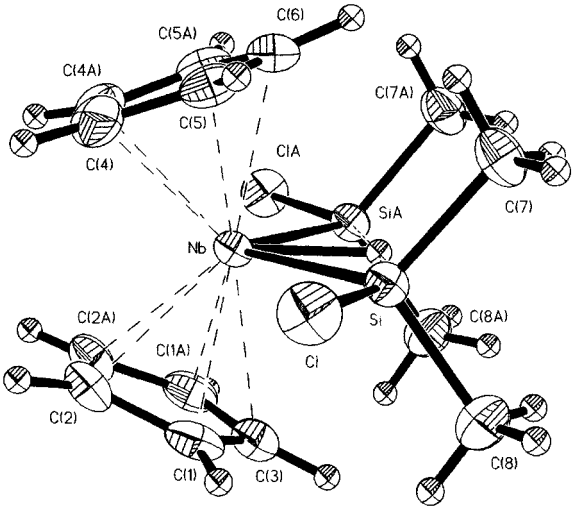

Figure 2. Molecular structure of **4**.

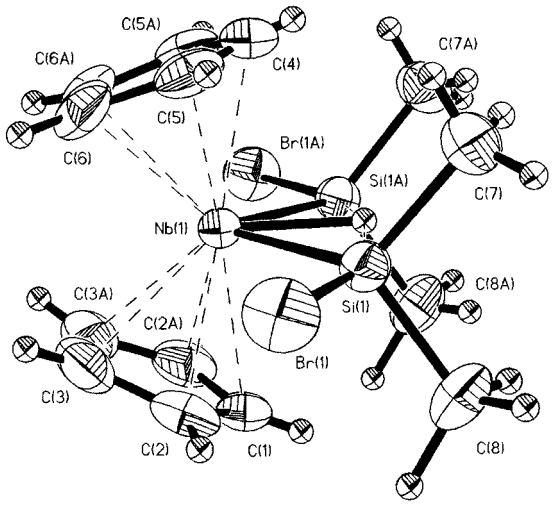

Figure 5. Molecular structure of **9**.

0947-6539/99/0510-2952 $ 17.50+.50/0 *Chem. Eur. J.* **1999**, *5*, No. 10

Table 1. Selected bond lengths [Å] and angles [°] in the niobocene silylhydrido complexes and related compounds.

Compound	Nb–Si	Si-Nb-Si(H)	Si–H	Reference
$[Cp_2Nb(SiFMe_2)_2H]$	2.618(1)	105.57(4)	1.980	this work
	2.622(1)			
$[Cp_2Nb(SiClMe_2)_2H]$	2.597(1)	104.27(5)	2.056	this work
$[Cp_2Nb(SiBrMe_2)_2H]$	2.604(2)	103.37(7)	2.053	this work
$[Cp_2Nb(SiClMe_2)H_2]$	2.579(2)	114.1	1.860	this work
$[Cp_2Nb(SiPhMe_2)_2H]$	2.654(1)	110.81(5)		this work
$[Cp_2Nb(SiMe_3)C_2H_4]$	2.669(1)			6e
$[Cp_2TaH_2SiMe_2Ph]$	2.651(4)			7g
$[Cp_2TaH(SiMe_2H)_2]$	2.624(2)	109.90(7)		5c
	2.633(2)			

Table 2. Comparison of the silicon–halogen bond lengths in silanes and in the niobocene silylhydrido complexes.

Compound	Si–X bonds in complexes [Å]	Si–X bonds in corresponding silanes $XSiR_3$ [Å]	Lengthening of the Si–X bond in complexes [Å]	Lengthening of the Si–X bond in complexes [%]
$[Cp_2Nb(SiFMe_2)_2H]$	1.652(3)	1.55	0.103	6.7
	1.644(3)			
$[Cp_2Nb(SiClMe_2)_2H]$	2.163(1)	2.02	0.143	7.1
$[Cp_2Nb(SiClMe_2)H_2]$	2.170(2)	2.02	0.15	7.4
$[Cp_2Nb(SiBrMe_2)_2H]$	2.349(2	2.15	0.199	9.3

called Bent's rule,[18] in which introduction of an electronegative substituent X in a compound $X–EY_n$ develops more p-orbital character of the central atom E in the X–E bond, leaving more s-orbital character for the bonds with substituents Y, and thus shortening them. Bent's rule predicts the shortest Nb–Si bond for the fluorine derivative **8**. However, comparison of the structure of **8** with that of the chlorine derivative **4** shows explicitly that the rehybridization effect does not operate alone. Thus, the Nb–Si bonds in **8** (2.618(1) and 2.622(1) Å) are about 0.025 Å *longer* than the Nb–Si bond in **4** ((2.597(1) Å)). Therefore, there must be an additional cause for the shortening of the Nb–Si bond, which is more pronounced in the chlorine derivative. The monosilyl complex **3b** exhibits an even shorter Nb–Si bond (2.579(2) Å). The striking properties of the chlorine complexes **3b** and **4** are also emphasized by the longer Nb–Si bond (2.604(1) Å) in the bromine complex **9**, which is still shorter than the corresponding bond in **8**, however. These trends suggest that there should be an additional electronic factor that contributes to the shortening of the Nb–Si bonds in this series of compounds and which increases in significance on moving down the halogen group, that is, from the fluorine derivative **8** to the bromine compound **9**. Superposition of this factor, which we call "interligand hypervalent interaction" (IHI), with the rehybridization effect creates a minimum for the chlorine complex **4** (Figure 6).

Another remarkable feature of **3b**, **4**, **8** and **9** is the variation of the silicon–halogen distances (Table 2). X-ray diffraction studies of transition metal complexes substituted by chlorosilyl ligands provide an ample field for comparison.[5d, 19, 20] Some complexes containing the moiety $M–SiR_2–F$ have also been characterized structurally.[21] The Si–Cl bonds in **3b** (2.170(2) Å) and **4** (2.163(1) Å) are the

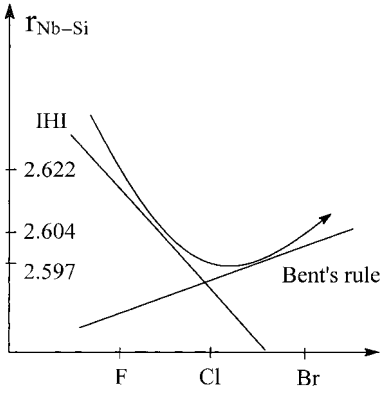

Figure 6. Schematic representation of how the contributions of Bent's rule and IHI lead to the shortening of the Nb–Si bond in $[Cp_2Nb(SiXR_2)_2H]$, and trends down the halogen group.

longest ones found for transition metal complexes with unhindered $SiClR_2$ (R = alkyl, aryl) ligands. Normally the "unperturbed" Si–Cl bond length for complexes $[L_nM–SiR_2–Cl]$ is within the range 2.149–2.094 Å.[19] The iridium complex $[(PMe_3)_2H_2Ir–SiCl(tBu)_2]$ exhibits an extremely long Si–Cl bond (2.187(4) Å) caused by the steric bulk of the $SiCl(tBu)_2$ fragment.[20] A fairly long Si–Cl bond (2.158(1) Å) was found in the unhindered molybdenum complex $[Cp_2MoH(SiMe_2Cl)]$.[5d] This lengthening was attributed to an interaction between the metal-based electron lone pair and the silicon–chlorine antibonding orbital, which develops silylene-like character at the silicon centre.[5d] Thus the Si–Cl bond length in complexes $L_nM–SiR_2–Cl$ depends on the nature of the transition metal M, the steric bulk, the electronic properties of the supporting ligands L and the nature of the substituents R on silicon. Unfortunately, no X-ray structure of a niobocene complex substituted by a chlorosilyl ligand, but without interligand Si–H interactions, is available for comparison. However, we think that the tungstenocene complex $[Cp_2W(SiMe_3)(SiiPr_2Cl)]$ can serve for this purpose.[5d] In it, the orientation of the $SiiPr_2Cl$ group does not allow any significant overlap between the metal-based electron lone pair and the Si–Cl antibonding orbital, and the Si–Cl bond is slightly lengthened (to 2.149(2) Å) by the unfavourable steric repulsion from the bulky isopropyl groups. Also, one can expect the d^2 tungstenocene moiety to be a better electron donor than the d^0 niobocene moieties of **3b** and **4**, thus further increasing the Si–Cl bond length in $[Cp_2W(SiMe_3)(SiiPr_2Cl)]$ in accordance with Bent's rule. Comparing the molecular structures of $[Cp_2W(SiMe_3)(SiiPr_2Cl)]$ and those of niobocenes **3b** and **4**, we must conclude that the relative lengthening of the Si–Cl bond in **3b** and **4** is caused by an additional electronic factor that can only be the interaction between the silicon and hydride ligands. The nature of this interaction will be discussed in the following section, where all the trends in structure and reactivity are explained from a unified viewpoint.

Only two complexes containing the fragment $M–SiR_2–F$ have been studied by X-ray diffraction analysis:[21] the manganese complex $[Cp'Mn(CO)_2(HSiPh_2F)]$ with an Si–F bond of 1.634(3) Å and the iron complex $[CpFe(CO)_2(SiPh_2F)]$ with an Si–F bond of 1.624(2) Å. In our complex

$[Cp_2NbH(SiMe_2F)_2]$ we observed long Si–F bonds (1.652(3) Å and 1.644(3) Å) for the two nonequivalent silicon centres. Although caution should be exercised in comparing complexes with substantially different supporting ligands, we believe that the difference in these bond lengths is caused to a great extent by an interligand interaction analogous to that in **3b** and **4**.

Our search of the Cambridge Crystallographic Data Centre did not reveal any transition metal complex with an SiR_2Br ligand. Thus, a direct comparison of the Si–Br distance in **9** with other bromosilyl derivatives has not been possible. However, the Si–X bond lengths in **3b**, **4**, **8** and **9** can be compared with the Si–X distances in the related silanes R_3Si–X; these data are summarized in Table 2. The relative lengthening of the Si–X bond is greatest in **9**. The short Nb–Si bond in the **9** is also consistent with an interligand interaction. Since two factors are responsible for the shortening of the Nb–Si bond, the fact that **9** has a longer Nb–Si bond than **4** does not mean that the interligand interaction in **9** is less than that in **3b** and **4**. The data in Table 2 are in accord with the latter possibility. The effect of rehybridization could be smaller, while shortening due to the interligand interaction could be even greater, and the observed bond length is the superposition of two opposite trends. In a series of similar silanes L–SiR_3–X (X = F, Cl, Br, I) with pentacoordinated hypervalent silicon atoms, the most significant lengthening of the Si–X bond was observed for X = Br, I.[22] The ability of the Si–X bond to participate in the hypervalent bonding thus increases down the halogen group.

Some of the most persuasive evidence in favour of the nonclassical nature of complexes **4**, **8** and **9** is provided by the values of the Si-Nb-Si bond angles (104.27(5)°, 105.57(4)° and 103.37(7)°, respectively). In the classical complex **6** the Si-Nb-Si angle is 110.81(5)°, although the steric bulk of the phenyl group is much greater than that of the fluorine substituent in **8**, for which the Si-Nb-Si bond angle (105.57(4)°) is surprisingly small. A larger Si-Ta-Si angle (109.90(7)°) was observed in the related tantalocene complex $[Cp_2Ta(SiHMe_2)_2H]$.[5c] In the crystal structures of other trisubstituted niobocenes, the lateral substituents L tend to maximize this angle L-Nb-L. In the dihydride derivatives, with the low steric requirements of the hydride ligands, H-Nb-H angles of about 120° were observed. However in other trisubstituted niobocenes, both hindered (such as $[Cp_2Nb(Hg(S_2CNEt_2))_3]$[23]) and relatively unhindered (such as $[Cp_2Nb(O_2)Cl]$[24]), bond angles greater than 120° were observed (124.4(1)° and 121.9(3)°, respectively). Recent theoretical consideration suggests that more electronegative lateral substituents L tend to increase the L-M-L bond angle;[25] this factor should contribute to the opening of the Si-Nb-Si bond angle in **4** in comparison with that in **6**. We can therefore conclude that in **4**, **8** and **9** the shifts of the silyl ligands towards the central position, which allow both the silicon centres to interact with the hydride ligand, are caused by additional electronic factors rather than steric ones.

The interaction between the silyl and hydride ligands results in fairly short Si–H contacts in **3b**, **4**, **8** and **9**. Schubert suggested that the shortest possible nonbonding contact between the Si and H centres is 2.0 Å.[2b] This value was calculated as half the sum of the shortest Si–Si distance in 1,3-disiloxanes,[26] believed to be nonbonding, and the shortest nonbonding H–H distance in the complexes of molecular hydrogen.[2b] However, it has been suggested that there is some sort of Si–Si bonding interaction (so-called unsupported π bonding) in 1,3-disiloxanes,[27] and therefore the range of this criterion should be expanded.[28] This has been recently emphasized by the discovery of a long Si–H bonding contact (2.1 Å) in a silane σ-complex.[29] In the chloro and bromo derivatives (**4** and **9**, respectively), two silicon centres are related by the crystallographically imposed mirror plane, the Si–H bond lengths are equal (2.056 Å in **4** and 2.053 Å in **9**) and the hydride interacts with *both* silicon atoms. These distances are considerably less than the sum of the van der Waals radii of the Si and H atoms (3.1 Å) and are shorter then the longest known Si–H bonding contact, cited above. In the fluorine compound **8** the two silicon centres are not related by symmetry and the short Si–H contact (1.9 Å) confirms unequivocally the bonding between the Si and H centres. The difference in the Nb–Si and Si–F bond lengths for the two nonequivalent silicon centres in **8** are at the limit of the accepted range of accuracy of the data. However, the observed trends in these values—the slightly shorter Nb–Si bond, the longer Si–F bond and the shorter Si–H contact for the central Si(1)—may also reflect a stronger interaction of this centre with the hydride ligand. If this difference is real, it can be explained easily by a second-order Jahn–Teller distortion in this complex (vide infra). In the monosilyl complex **3b**, in which the hydride ligand interacts with only one silyl ligand, a short Si–H contact (1.86 Å) was found which is very close to the "normal" Si–H distance range (1.75–1.80 Å) usually observed in silane σ-complexes.[2b]

To summarize, the nonclassical interligand interaction in complexes **3a**, **4**, **8** and **9** results in four main structural trends: i) the metal–silicon bonds are shorter than those normally observed; ii) the silicon–halogen bonds are longer than normal; iii) Si–H contacts are present; and iv) in the bis(silyl) complexes the observed Si-Nb-Si bond angles are smaller than expected. In contrast, the description in terms of 3c–2e interactions of silanes with transition metals predicts long Si–M bonds and gives no rationale for the Si–X bond lengths.[2b,c] This description also fails to explain the *trans* position of the hydride and halogen substituents at silicon. Therefore, we conclude that complexes **3b**, **4**, **8** and **9** are not silane σ-complexes and an alternative theory is required to explain the interligand interactions in these compounds.

The theory of interligand hypervalent interactions: A hint on the origin of interligand interactions in complexes **3b**, **4**, **8** and **9** comes from the molecular structures shown in Figures 1, 2, 4 and 5. In all four compounds the silyl ligands are oriented so that the halogen substituents are located strictly in the bisecting plane of the Cp_2Nb moiety *trans* to the hydride ligands. Coupled with the close proximity of the silyl and hydride ligands, such an orientation should provide an overlap between the Nb–H bonding orbital and the X–Si σ*-antibonding orbital (see structure **A**, Figure 7 bottom). Population of the latter causes lengthening of the Si–X bond. For the monosilyl complex **3b**, where the hydride ligand interacts with only one silyl ligand, Figure 7 bottom is the orbital

  0947-6539/99/0510-2954 $ 17.50+.50/0 *Chem. Eur. J.* **1999**, *5*, No. 10

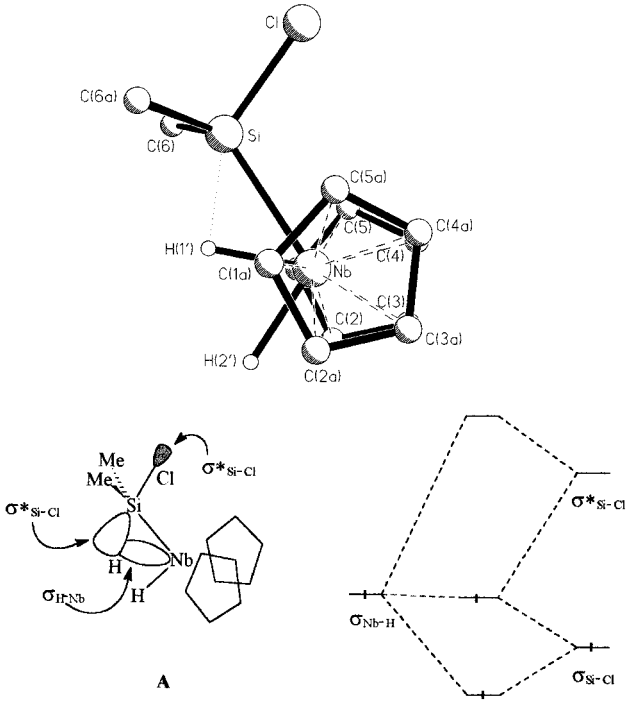

Figure 7. Top: View on the bisecting plane of **3b**. Bottom: Orbital interaction diagram for the interligand interaction in complex **3b**.

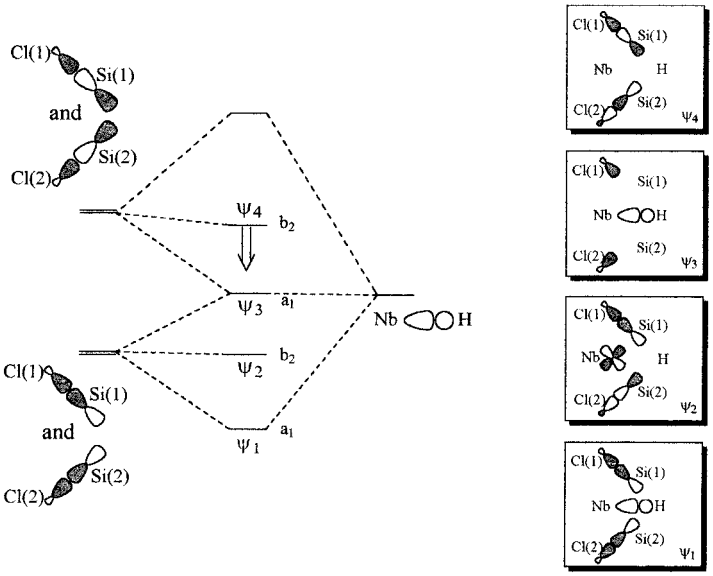

Figure 8. Qualitative orbital interaction diagram for the interligand interaction in complexes **4**, **8** and **9**. The down-arrow shows how the energy of Ψ_4 is reduced on replacing Cl in **4** for F in **8**.

interaction diagram; it is a typical diagram describing the bonding in hypervalent compounds. The hydride and halogen substituents occupy the apical positions around the silicon atom while the methyl groups and niobium atom form the equatorial plane. As is typical for hypervalent compounds, the resulting distorted trigonal-bipyramidal geometry of silicon causes "rehybridization" of the silicon atom, thus giving more Si s-orbital character to the Nb–Si bond, and shortening it.[30] More p-orbital character goes into the bonding with the halogens, making the Si–X bonds longer. In the bis(silyl) compounds **4**, **8** and **9** the hydride ligand interacts with both silyl groups, and the orbital interaction diagram is more sophisticated: the interaction of the Nb–H bonding orbital with the symmetrical combinations of the Si–X bonding and antibonding orbitals is supported by mixing with appropriate niobium orbitals (Figure 8). As a result, we have five-centre Cl-Si-H-Si-Cl bonding provided by six electrons (two pairs from the Si–X bonds, and the Nb–H pair) and this interaction occurs within the coordination sphere of niobium. Both silicon centres adopt a distorted trigonal-bipyramidal geometry, with the hydride ligand occupying the apical position of both. This theoretical description suggests that it may be more appropriate to consider the Nb–H bond as a whole to be the apical substituent at silicon. To the best of our knowledge, this is the first time that a σ bond has been found to serve as an apical substituent X in a hypervalent compound X–ER$_n$–Y.

Hypervalent bonding in compounds X–ER$_n$–Y is frequently considered as a model for the nucleophilic substitution process at the element E.[22] Analogously, our proposed interligand hypervalent interaction in transition metal hydridosilyls can be relevant to the initial stages of hydrogen migration onto the silyl ligands.

As discussed in the previous section, the fluorine complex **8** has nonequivalent silicon centres, the difference between them being at the limit of the accepted range of accuracy. We cannot yet be sure whether the observed differences are the result of inaccuracy in data or represent the presence of additional minor electronic effects. It is noteworthy, however, that the observed trends in three parameters (a shorter Nb–Si bond, a longer Si–F bond and a shorter Si–H contact) are consistent with the latter possibility; they could be a result of weak second-order Jahn–Teller distortion in **8**, caused by the lower position of the Si–F antibonding orbitals due to the high electronegativity of the fluorine substituent.[32] It is well known that increased electronegativity of atom X pushes the E–X antibonding orbital down in energy.[32a] In **8** the asymmetric combination of the Si–F antibonding orbitals, having b_2 symmetry, lies closer to the HOMO (symmetry a_1) than in **4** and **9**, and therefore can interact with the B_2 vibration mode, creating second-order Jahn–Teller distortion. As a result of this distortion, the hydride ligand in **8** may have stronger interligand hypervalent interaction with the Si(1) centre. The equivalence of $SiMe_2$ groups in the ^{1}H NMR spectrum even at low temperatures (down to $-80\,^\circ$C) is then easily explained by the tunnelling movement of hydride between the two centres.

Ab initio calculations: To gain a deeper insight into the nature of interligand interactions in the halosilyl niobocene complexes, ab initio calculations of a series of model compounds were carried out. We chose density functional theory as it has been demonstrated to be an economic but useful method for the study of relatively large organometallic compounds.[33] The performance of the chosen method for the species under study was tested by geometry optimization of the real complex **3b**. Its structure (Figure 9) exhibits reasonable agreement with the crystallographically determined structure (see Figure 1). Particularly noteworthy are the positions of the hydride ligands, for which X-ray crystallography may give

unreliable values. The calculated Nb–H bond lengths in **3b** (1.745 and 1.793 Å for the lateral and central hydrides, respectively) can be compared with the corresponding X-ray results (1.766 and 1.669 Å). The Nb–H bond lengths in $[Cp_2NbH_3]$, determined recently by NMR relaxation techniques, range between 1.78 and 1.81 Å,[34] so the superiority of the calculated results is apparent. The main discrepancies between the calculated and observed structures of **3b** are the longer Nb–Si and Si–Cl bonds in the former: 2.632 Å versus 2.579(2) Å and 2.216 Å versus 2.170(2) Å, respectively. In the previous calculations of transition metal silyl complexes both shorter and longer M–Si bonds were observed, although elongation of the calculated bonds appears to be a more general phenomenon.[35] Since relatively weak bonds are known to be generally shorter in the solid state than in the gas phase, the 0.05 Å difference between the calculated and crystallographically determined Nb–Si bond length can be partially accounted for by crystal packing effects. However, for determining trends rather than absolute values, the present level of calculation was considered satisfactory. In further calculations we made the usual substitution of the methyl groups on silicon by hydrogen atoms, which allowed us to calculate a series of model mono- and bis(silyl)complexes $[Cp_2NbH_{3-m}(SiH_nCl_{3-n})_m]$ ($m = 1, 2$; $n = 2, 3$) (**11**–**16**). The optimized geometries with the most important bond lengths and angles are shown in Figure 9.

The trends exhibited by the calculated structures **11**–**16** are in perfect agreement with our observations of the X-ray structures. Thus, the Nb–Si bond lengths found for the chlorosilyl complexes **11**–**13** are shorter than those in the SiH_3 complexes, in agreement with Bent's rule. Also, the Nb–Si bond (2.581 Å) in the asymmetric complex **11** is shorter than the corresponding bond in **12** (2.600 Å), which is a manifestation of stronger IHI in **11**. The Si–Cl bond (2.195 Å) in **11** is longer than that in **12** (2.177 Å), paralleling analogous trends in the Nb–Si and Si–Cl bonds found for the crystal structures of **3b** and **4**. The most interesting point is that the "symmetric" monosilyl complex **13** was also found to possess IHI: the optimized structure turned out to be asymmetric, in that a shorter contact was found with one of the lateral hydride ligands (2.097 Å versus 2.487 Å), whereas the values for the Nb–Si and Si–Cl bonds were close to those observed in **12**. It is important to note that in calculating complex **13** we started with a C_1 structure, with the silyl ligand located symmetrically between two hydrides and the chlorine substituent at silicon oriented out of the bisecting plane. During the optimization procedure, the chlorine atom came exactly into the bisecting plane, *trans* to one of the hydride ligands, and the silyl group moved closer to this "interacting" hydride.

To study further the importance of the *trans* orientation of the halogen atom with respect to the hydride, the geometry optimization of a conformer of **3b** with the *cis* orientation of the Si–Cl and Nb–H^1 bonds (**3b′**) was performed. The optimized structure of **3b′** is shown in Figure 9. Energetically, **3b′** is 11.0 kcal mol^{-1} less stable than **3b**. However, this fact alone does not support the existence of any specific interaction in **3b** because the steric preferences may differ substantially in the two isomers; however, such a large difference between the two conformations can hardly be caused by steric effects alone. More important for our analysis of the Si–H interaction are the geometric differences between **3b** and **3b′**. Compared with **3b**, **3b′** exhibits a much longer (by nearly 0.1 Å) Si–H^1 distance, which parallels the shortening of the Nb–H^1 bond in **3b′** ($\Delta(Nb–H^1) = 0.04$ Å) while the Nb–H^2 bond remains almost unaltered. These findings are in accord with a smaller electron withdrawal from the Nb–H^1 bond in **3b′**. Simultaneously, a very long Nb–Si bond (2.713 Å) in **3b′** is observed, while the Si–Cl bond length is shortened by 0.016 Å. Although the geometric parame-

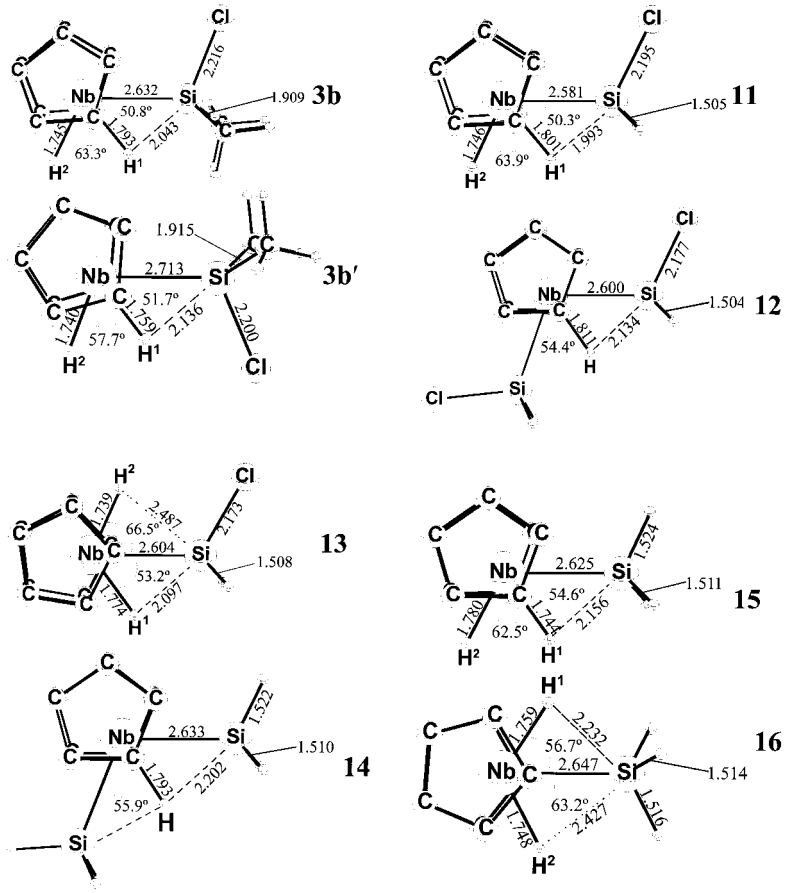

Figure 9. Geometries of the complexes **3b** and **11**–**16** optimized at the BP86 level. Hydrogen atoms of the Cp rings are omitted for clarity.

0947-6539/99/0510-2956 $ 17.50+.50/0 *Chem. Eur. J.* **1999**, *5*, No. 10

ters in **3b′** are affected by the increased steric repulsion of the Si–Cl bond from the Nb–H[1] bond, all the changes in these parameters on going from **3b** to **3b′** conform perfectly with the disappearance of the σ(Nb–H) $\rightarrow\sigma$(Si–Cl)* donation in **3b′**. The importance of the *trans* orientation of the Si–X bond to the interacting hydride is hereby confirmed.

The isomer **11** was found to be 1.4 kcal mol^{-1} more stable than **13**, in perfect agreement with the value observed from the NMR experiments for **3b** and **3a** (0.5 kcal mol^{-1}). It appears that there is a weaker IHI in the SiH_3 complexes too. Thus, analogous asymmetry in the "symmetric" monosilyl isomer **16** was observed, with one Si–H contact being shorter than the other (2.232 Å versus 2.427 Å). The existence of IHI in the SiH_3 complexes is further supported by the fact that one of the Si–H bonds is oriented *trans* with respect to the hydride and is longer than the other two; the difference exceeds 0.01 Å for **14** and **15** but is very small for the central SiH_3 complex **16**. Overall, the Si–H contacts found for the SiH_3 complexes **14**–**16** are longer than those in the chlorosilyl complexes (2.153–2.232 Å versus 1.993–2.133 Å), in accordance with the stronger IHI in the latter. Also, the weakness of the Si–H interaction in the SiH_3 complexes is emphasized by the *lower* (by just 0.6 kcal mol^{-1}) stability of **15** compared with **16**, which is an opposite trend to that in their chlorinated analogues **12** and **13**. It appears that hydrogen is the "boundary" substituent on silicon, for which nonclassical silicon–hydride hypervalent interaction is possible. More electropositive groups, such as methyl, do not cause this type of nonclassical interaction. In this context, Buchwald's complex [$Cp_2Ti(PMe_3)(SiH_2Ph_2)$] is relevant; its structure was referred to as intermediate between the classical silyl hydride and silane σ-bond complexes.[7d] In this compound the hydrogen directly bonded to silicon and the "hydride" occupy the apical positions relative to the silicon centre, with Si–H bond lengths of 1.56(5) and 1.69(5) Å, respectively. The former value is greater than the normal Si–H bond length (1.47 Å) observed in silanes, but is in good agreement with the values found in our calculations (in the range 1.516–1.522 Å). Analogous *trans* geometry, signifying IHI, was also observed in the tantalum bis(silyl) complex [$Cp_2TaH(SiHMe_2)_2$].[5c] The Si-Ta-Si bond angle observed for this compound (109.9(7)°) is slightly smaller than the corresponding angle in the much bulkier complex [$Cp_2Nb(SiPhMe_2)_2H$] (110.81(5)°). It therefore appears that these titanium and tantalum compounds may have weak IHI between the silyl and hydride ligands.

The nature of the Si–H interactions in complexes **11**–**16** was elucidated by natural bond orbital (NBO) analysis[36] and topological analysis of the electron density based on Bader's atom-in-molecule theory.[37] The NBO analysis results are summarized in Table 3, where the Wiberg bond indices are also given. The NBO analysis did not reveal any Si–H bond in the complexes under study, because this interaction is too weak to be found as a bond within standard NBO program thresholds. Nonetheless, important conclusions can be drawn from the properties of Nb–H, Nb–Si and Si–X NBOs. From Table 3, the occupancy of the Nb–Si bond in the chlorosilyl complexes **11**–**13** is higher than in the corresponding SiH_3 complexes **14**–**16**, yet in all cases it is significantly less than 2. Both the NBO bond orders and Wiberg bond indices show higher Nb–Si bond orders for the chlorosilyl complexes **11**–**13** than for **14**–**16**. Simultaneously, the Si–X bond orders are lower for **11**–**13** (X = Cl) than for **14**–**16** (X = H), while the occupancy of the Si–Cl antibonding orbitals is higher than the occupancy of the Si–X* (X = H) antibonding orbitals. These data demonstrate that IHI is stronger in the chlorosilyl complexes and results in stronger Nb–Si and weaker Si–X bonds. Also, the Nb–Si bonds in **11**–**13** have more Si s character than the Nb–Si bonds in **14**–**16**, whereas the Si–X bond has less Si s character. Both of these facts are in perfect agreement with Bent's rule and the strength of IHI.

The characteristics of the interacting and noninteracting Nb–H bonds are significantly different. The bond orders and occupancy of the interacting Nb–H bonds are lower than for the noninteracting ones. Occupancy of the latter is quite close to 2, while the former are apparently electron-deficient. Again, the bond orders and occupancy of the interacting Nb–H bonds in the chlorosilyl complexes **11**–**13** are lower than those in **14**–**16**.

The lack of electrons in the Nb–H bonding NBO, in conjunction with the significant population of the σ(Si–X)* antibonding NBO, suggests the occurrence of electron transfer from the former to the latter. The occupancy of the σ(Si–H)* NBO is much lower than that of the Si–Cl* bond, which is in line with stronger IHI in chlorosilyl complexes.

The data of Table 3 are in accord with electron transfer from the σ(Nb–H) bond orbital into the σ(Si–Cl)* antibonding orbital. We also found significant Wiberg bond indices for the nonclassical Si–H contacts for complexes **11**–**16**. The highest value (0.228) was observed for the monosilyl complex **11**; this parallels the observed trends in other parameters and

Table 3. Results of the natural bond orbital analysis of the niobium silyl hydride complexes **11**–**16** at BP86 level of theory.

Molecule	Nb–Si bond					Si–X bond					Nb–H[1] [a]		Nb–H[2] [a]		Si–H[1] [a]	Si–H[2] [a]
	bond order[b]	occ.[c]	Si [%]	s [%]	p [%]	bond order[b]	occ.[c]	Si [%]	s [%]	p [%]	bond order[c]	occ.[c]	bond order[b]	occ.[c]	bond order [b]	bond order[b]
11	0.57/0.68	1.78/0.30	42.6	34.8	64.7	0.59/0.72	1.98/0.12	22.4	13.6	84.7	0.45/0.57	1.70/0.19	0.51/0.75	1.90/0.30	0.31/0.23	0.01/0.01
12	0.55/0.68	1.80/0.25	43.4	33.9	65.8	0.60/0.75	1.98/0.09	22.9	15.2	83.2	0.44/0.54	1.68/0.28	–	–	0.24/0.17	-
13	0.54/0.63	1.74/0.27	45.9	35.2	64.5	0.61/0.76	1.98/0.09	23.2	15.7	82.7	0.49/0.66	1.79/0.21	0.52/0.72	1.87/0.20	0.26/0.18	0.15/0.10
14	0.52/0.66	1.79/0.23	43.4	30.8	68.8	0.75/0.91	1.98/0.04	40.4	21.4	77.5	0.46/0.57	1.70/0.27	–	–	0.21/0.15	-
15	0.53/0.66	1.77/0.23	44.8	31.3	68.4	0.75/0.90	1.97/0.05	40.3	20.8	78.1	0.47/0.62	1.76/0.23	0.51/0.75	1.89/0.18	0.24/0.17	0.00/0.01
16	0.51/0.61	1.72/0.24	46.6	32.0	67.7	0.75/0.91	1.98/0.03	40.5	22.8	76.3	0.51/0.69	1.81/0.20	0.52/0.72	1.87/0.19	0.20/0.14	0.16/0.11

[a] H^1 is the hydrogen closest to Si, H^2 is the hydrogen farthest to Si. [b] Atom–atom overlap-weighted NAO bond order and Wiberg bond indices are separated by slash. [c] Occupation of bonding and antibonding NBOs are separated by slash.

the results of X-ray structure determination of the corresponding complex **3b**. In summary, conclusions about the following interactions between NBOs can be drawn from Table 3: there is σ(Nb–H) $\rightarrow\sigma$(Nb–Si)* electron transfer, which is apparently intrinsic for all the complexes under study and is relatively independent of the nature of the silyl moiety. This transfer was described by Hübler et al. for osmium–silyl complexes.[38] Further, there is σ(Nb–H) $\rightarrow\sigma$(Si–X)* interaction, which depends crucially on the nature of the substituent X and is substantially stronger for X = Cl than for X = H. A significant population of the σ(Nb–H)* antibonding NBO can be accounted for by the σ(Nb–Si) $\rightarrow\sigma$(Nb–H)* back-donation.

Within the framework of Bader's atoms-in-molecules theory, a "bond path" (a line along which the magnitudes of electron density $\rho(\boldsymbol{r})$ are maximal with respect to any infinitesimal lateral displacement) corresponds to a chemical bond. In our study, the bond path between Si and H atoms was found only for **3b** and **11**, that is, for the molecules with the strongest IHI, according to the bond lengths and NBO results. This bond path is strongly curved towards the Nb atom. Analogously, a significantly curved Si–H bond path was found for the agostic Ti ← H–Si interaction.[33a] Formally, there must be a bond path between any chemically bonded atoms. Sometimes, however, a bond path may exist between repulsively interacting atoms located close to each other.[39] In a series of related molecules a bond path can arise as two interacting atoms come closer to each other. This process can be described rigorously in terms of the catastrophe theory.[37] Apparently, the Si–H bond path in **3b** and **11** is close to collapsing to give the Nb–Si and Nb–H paths; these paths exist for the other complexes **12**–**16**, for which no Si–H bond path is found. Hence, the Si–H interaction under discussion is a weak one. This is further supported by an enormously high ellipticity of the Si–H bond critical point in **11** (Table 4). Nevertheless, important indirect conclusions can be drawn on the basis of the properties of critical points corresponding to other bonds, such as Nb–Si, Nb–H, and Si–Cl. Relevant data are given in Table 4. Attention should be paid principally to the Nb–H bond critical points. In **11** and **13**, the electron density $\rho(\boldsymbol{r}_c)$ for the Nb–H^1 bond is clearly lower than for the Nb–H^2 bond, which is in the expected agreement with the longer Nb–H^1 bond. Simultaneously, however, the density Laplacian $\nabla^2\rho(\boldsymbol{r}_c)$ is much more positive for the Nb–H^1 bond. Since, according to Bader,[37, 40] $\nabla^2\rho$ is negative in areas of relative electron concentration and positive in areas of relative electron depletion, the smaller $\rho(\boldsymbol{r}_c)$ along with greater positive $\nabla^2\rho(\boldsymbol{r}_c)$ indicates an electron *withdrawal* from the Nb–H^1 bond. The energy density $H(\boldsymbol{r}_c)$, which was proposed as an alternative criterion of electron concentration/depletion and bond covalency,[41] is less negative for the Nb–H^1 bond—in line with the Laplacian. The SiH_3 complexes **15** and **16** exhibit the same trend, but in this case the difference between the Nb–H^1 and Nb–H^2 bonds is less pronounced. These data agree perfectly with the weaker IHI for the SiH_3 complexes. Nevertheless, even in the complex **16**, $\nabla^2\rho(\boldsymbol{r}_c)$ differs markedly for the Nb–H^1 and Nb–H^2 bonds. Among the complexes **11**–**16**, the bis(chlorosilyl) complex **12** possesses the lowest Nb–H $\rho(\boldsymbol{r}_c)$ and the most positive $\nabla^2\rho(\boldsymbol{r}_c)$.

Table 4. Results of the topological analysis of the electron density in the niobium silyl hydride complexes **11**–**16** at BP86 level of theory.[a]

Molecule	Bond	$\rho(\mathbf{r}_c)$	$\nabla^2\rho(\mathbf{r}_c)$	$H(\mathbf{r}_c)$	ε_c
11	Nb–Si	0.4742	–0.0991	–0.1716	0.2765
	Nb–H^1	0.6209	3.0922	–0.1934	0.1992
	Nb–H^2	0.7444	1.7923	–0.2779	0.1126
	Si–Cl	0.5005	2.9150	–0.2169	0.0645
	Si···H^1	0.4068	0.1617	–0.1183	1.4361
12	Nb–Si	0.4691	–0.1774	–0.1681	0.2287
	Nb–H	0.5995	3.4238	–0.1805	0.2480
	Si–Cl	0.5155	3.3127	–0.2197	0.0571
13	Nb–Si	0.4562	0.0793	–0.1581	0.2587
	Nb–H^1	0.6792	2.6038	–0.2317	0.1695
	Nb–H^2	0.7567	1.8035	–0.2875	0.1141
	Si–H	0.7635	2.7388	–0.4245	0.0477
	Si–Cl	0.5178	3.4242	–0.2189	0.0228
	Si–H	0.7634	2.7377	–0.4245	0.0478
14	Nb–Si	0.4465	–0.3156	–0.1587	0.2354
	Nb–H	0.6374	3.0057	–0.2075	0.1775
15	Nb–Si	0.4496	–0.2915	–0.1601	0.2143
	Nb–H^1	0.6641	2.5962	–0.2253	0.1328
	Nb–H^2	0.7448	1.8398	–0.2781	0.1224
16	Nb–Si	0.4301	–0.0706	–0.1461	0.2308
	Nb–H^1	0.7113	2.2296	–0.2553	0.1364
	Nb–H^2	0.7375	1.9834	–0.2732	0.1253
	Si–H^{trans}	0.7344	3.0227	–0.3925	0.0267
	Si–H	0.7367	2.8992	–0.3987	0.0117

[a] Electron density at the bond critical points $\rho(\mathbf{r}_c)$ (e Å^{-3}), Laplacian of electron density at the bond critical point $\nabla^2\rho(\mathbf{r}_c)$ (e Å^{-5}), electron energy density $H(\mathbf{r}_c)$ (Hartree Å^{-3}), and ellipticity ε_c ($\varepsilon_c = \lambda_1/\lambda_2 - 1$, where λ_1 and λ_2 are negative eigenvalues of electron density Hessian).

The electron withdrawal from this Nb–H bond is strengthened by two accepting SiH_2Cl groups.

The properties of the Si–Cl bonds in **11**–**13** are also noteworthy. The values of $\rho(\boldsymbol{r}_c)$ increase only slightly from **11** to **12** and are almost identical in **12** and **13**, which agrees well with the Si–Cl bond lengths. Contrarily to the Nb–H bonds, $\nabla^2\rho(\boldsymbol{r}_c)$ varies in line with $\rho(\boldsymbol{r}_c)$. This suggests that an elongation of the Si–Cl bonds does not lead to significant electron depletion in the bond region. Hence, there must be some compensation for an unavoidable decrease in density owing to increasing Si–Cl separation, which can be provided by a donation to the Si–Cl* bond.

Following the suggestion of a referee, we examined the dependence of the total energy and the geometry of **3b** on the position of the H^1 hydride ligand in the bisecting plane of the niobocene moiety. To this end, a series of constrained geometry optimizations of the distorted complex **3b** were performed, keeping the Si-Nb-H^1 and H^1-Nb-H^2 angles fixed and allowing all other geometrical parameters to relax. When the Si–H^1 separation was artificially shortened, the IHI was expected to be forcibly increased, at least at moderate distortions. Similarly, IHI was expected to decrease at longer Si–H^1 distances.

The changes in the most important bond lengths are shown in Figure 10. With increasing Si–H^1 separation, the Si–Cl bond shortens and the Nb–Si bond elongates, which is in accord with weakened IHI. As H^1 approaches H^2, both Nb–H^1 and Nb–H^2 bonds elongate, after initial slight shortening. This is most probably a result of an H^1–H^2 interaction. Whether it

0947-6539/99/0510-2958 $ 17.50+.50/0 *Chem. Eur. J.* **1999**, *5*, No. 10

is repulsive (closed-shell) or attractive (starting to form a dihydrogen complex) is not clear, although we favour the latter possibility since the previous calculations on Cp_2NbH_3 showed the formation of a dihydrogen state on analogous movement of the central hydride.[42] In the opposite direction, as H^1 approaches silicon (in the negative part of the graph, Figure 10), it is the Nb–Si bond that experiences most significant changes. It elongates by more than 0.2 Å at 20° distortion and more than 0.1 Å at 15° distortion of the Si-Nb-H^1 angle. Apparently, such a strong effect at large distortions is caused merely by Si–H repulsion. The Nb–H^1 distance increases strongly at moderate distortions, which is in line with a stronger IHI, but shortens slightly at very large distortions. Similarly, the initial elongation of the Si–Cl bond length is followed by its substantial shortening at large distortions. These geometrical changes at high distortions may reflect the forcible formation of a silane σ-bond complex, which in the initial stages of oxidative addition of an Si–H bond (that is, in the late stages of reductive elimination) is supposed to coordinate to a metal through the hydrogen atom.[2b, 43] To sum up, the geometric changes that occur when H^1 wanders between H^2 and Si agree well qualitatively with the concept of the dependence of IHI on the Si–H^1 distance superimposed by the Si–H^1 and H^1–H^2 repulsions when the respective atoms approach each other very closely.

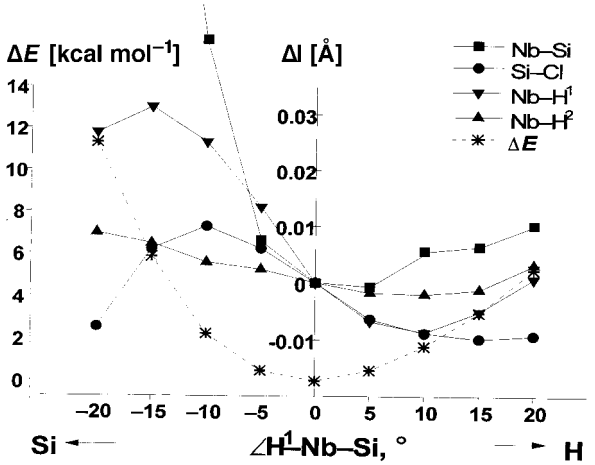

Figure 10. Dependence of the relative energy ΔE [kcal mol^{-1}] and geometrical parameters Δl [Å] on the deviation of the H^1-Nb-Si bond angle [°] from equilibrium. Negative deviations correspond to motion of H^1 towards Si, positive deviations to motion of H^1 towards H^2. The BP86 method was used for calculations. The basis set is described in the text.

Fan and Lin have recently calculated, at the MP2 level of theory, a series of niobocene bis(silyl) $[Cp_2NbH(SiH_{3-n}Cl_n)_2]$ ($n=0$, **A**; $n=1$, **B**; $n=2$, **C**; $n=3$, **D**) and mono(silyl) complexes $[Cp_2NbH_2(SiH_{3-n}Cl_n)]$ ($n=0$, **a**; $n=1$, **b**; $n=2$, **c**; $n=3$, **d**) and performed qualitative analysis of Laplacian maps.[44] Complexes **A**, **B**, **a** and **b** are analogous to our model compounds **14**, **12**, **15** and **11**, respectively. These authors recognized the hypervalent environment of silicon centres and the peculiar role of the "in-plane" chlorine atom, but they did not observe bond paths in **A – D** and **a – d**, and regarded complexes **A – D** as "classical silyl – hydridosilyl complex(es), with significant polarizing interactions of the silyl ligands for the central hydride". Similarly, **a – d** were regarded as "totally classical dihydride and hydrido – silyl systems". However, our observation of a bond path for complex **11**, or **b**, suggests that the results of analysis of Laplacian maps can depend on the level of calculation and that care should be taken in making deductions based only on the qualitative analysis of Laplacian maps. In our study it was essential that we used DFT theory with correlated electron density. Furthermore, the analysis of structural trends for **A – D** and **a – d** is totally in accord with our conclusions and the presence of IHI in these compounds (see Tables 1 and 3 in ref. [44]). Indeed, a geometrical restriction was imposed in the calculations of **C** and **c** (see Computational Details in ref. [44]), which prevented the chlorine substituent from going into the bisecting plane of the niobocene moiety. As a result, the case $n=2$ (**C** and **c**) is an exception from both series, with the Nb–Si bonds and Si–H contacts being longer than for the cases $n=1$ (**B** and **b**) and $n=3$ (**D** and **d**) (Nb–Si bond: 2.589 Å in **C** versus 2.588 Å in **B** and 2.564 Å in **D**; Si–H contact: 2.200 Å in **C** versus 2.154 Å in **B** and 2.147 Å in **D**). In addition, in **C** and **c** the angles Si-Nb-Si and Si-Nb-H, respectively, are about 2° larger than for the cases $n=1, 3$. Unfortunately, the Si–Cl bond lengths were not given for **C** and **c**. These trends show clearly that changing the geometrical parameters along the series **A – C** and **a – b** is not the result of increasing the number of chlorine substituents only (a manifestation of Bent's rule), but clearly there is also another electronic factor that is absent (or is very weak) in **C** and **c**, in which the chlorine atoms lie out of bisecting plane and IHI is present only in the weak form H–Si–H (vide supra). Therefore, considering **A – D** and **a – d** as silyl hydrides in the d^0 configuration is a reasonable starting point for discussing the interligand interaction therein, but regarding these complexes as "totally classical" is a simplification of the real bonding situation.

NMR studies: Some of the strongest evidence in favour of a silane σ-complex is provided by the observation of large Si,H coupling constants. After analysis of the data for a series of silane σ-complexes, it was proposed that a coupling constant of not less than 20 Hz may be associated with a direct Si–H interaction in such complexes.[2b] The numerous experiments that were performed to determine the Si,H coupling constants in our niobocene silyl compounds **1 – 9**, including low-temperature and inverse silicon–hydrogen heteronuclear correlation techniques, all failed to reveal any Si–H coupling constants. The presence of the strongly quadrupolar ^{93}Nb nucleus (nuclear spin ½) results in broad hydride and silicon resonances even at temperatures down to −100 °C. Consequently, measurement of the Si,H coupling constant was not possible. Nor was any coupling observed in the inverse Si – H heteronuclear correlation experiment; this could be caused either by the presence of the ^{93}Nb nucleus or the coupling constant being very close to 0. The latter possibility is very unrealistic since normally $^2J_{Si,H}$ couplings of about 7 – 10 Hz are easily observed.

Although no data for $J_{Si,H}$ in our niobocene complexes are available at the moment, we expect them to be relatively

small, probably of the order of $^2J_{Si,H}$. If the bonding between H and Si atoms in niobocenes **3b**, **4**, **8** and **9** is caused by overlap between the Nb–H bond orbital (mainly of hydrogen s character) and the Si–Cl antibonding orbital that has mainly silicon p character (note also that only the diffuse p orbital of Si can provide an essential overlap with the s orbital of H), then the Si–H coupling due to the direct interaction should be small. In contrast, in the silane σ-complexes the direct Si–H interaction stems essentially from the overlap of the s electrons from both Si and H. This is why a large coupling is observed.

Some NMR trends in the Group 5 metallocene silyl hydride complexes provide indirect evidence in favour of nonclassical interactions. Thus, in the ^{1}H NMR spectra of **2**–**6** the bis(silyl) hydrides bearing only alkyl and aryl substituents at silicon exhibit a downfield hydride resonance with respect to the corresponding dihydridosilyl complexes $[Cp_2M(H)_2SiR_3]$ ($\delta = -3.23$ in **6** versus $\delta = -4.79$ in **2**), while an opposite trend is observed in the chloro-substituted silyl complexes ($\delta = -5.15$ in **4** versus $\delta = -4.80$ in **3a**). The upfield shift of a hydride signal is often associated with the formation of a hydride bridge; thus the spectral peculiarities of **4** could be interpreted in terms of some kind of bonding between hydride and silicon centres. Also, in the nonclassical **3b** the broad resonance at $\delta = -4.63$ due to the central hydride ligand comes upfield relative to the signal of the lateral hydride ($\delta = -4.42$), whereas the reverse situation is observed for $[Cp_2NbH_3]$. Some minor trends in the position of signals of other groups in **3a** and **3b** are also suggestive of a larger electron density shift from the Cp rings towards the Me groups at Si in **3b**. Thus, the Cp resonance in **3a** is shifted upfield relative to the corresponding resonance in **3b** ($\delta = 4.61$ versus $\delta = 4.69$), while the opposite is observed for the Me signals ($\delta = 0.91$ versus $\delta = 0.80$). For each compound these values were obtained from the same sample, under identical conditions.

To summarize, although the NMR data provide some indirect evidence in favour of the nonclassical nature of **3b** and **4**, proper correlation of the structural parameters with the NMR data is still required. This will probably be possible after investigation of the proposed silicon–hydride interaction in other metal systems and with other supporting ligands.

Conclusion

The structure and reactivity trends obtained for the mono- and bis(halosilyl)-substituted niobocene hydrides suggest the presence of nonclassical interligand interactions between the silyl and hydride ligands. The trends observed are the opposite of those predicted by the common 3c–2e σ-complex theory. Therefore we have suggested an alternative theory of interligand hypervalent interaction. The main idea is that the interligand interaction emerges because of the transfer of electron density from the electron-rich M–H bond into the Si–X (X = halide) antibonding orbital. This kind of bonding can be described as 4c–4e interaction in the case of mono(silyl) complex **3b** and 6c–6e (or 5c–6e in the coordination sphere of the niobium atom) in the case of bis(silyl) complexes **4**, **8** and **9**. The electron/centre ratio is 1 for **3b**, **4**, **8** and **9**, which is higher than the corresponding ratio (0.66) for the 3c–2e σ-bond complexes, and therefore the former kind of interligand interaction can be described as electron-rich. The main structural trends due to IHI are: i) the metal–silicon bonds are shorter than those normally observed, ii) the silicon–halogen bonds are longer than normal, iii) Si–H contacts are present and iv) in the bis(silyl) complexes the observed Si-Nb-Si bond angles are smaller than expected. The silane σ-complex description fails to explain these trends. In the bis(silyl) complexes **4**, **8** and **9** the hydride ligand interacts with both silicon centres, which is inconsistent with the σ-bond complex bonding scheme. The complex with the strongest IHI is the monosilyl complex **3b**, in which the hydride has an interaction with only one silicon centre. Not surprisingly, this compound has the longest Si–Cl bond, the shortest Nb–Si bond and the shortest Si–H contact. Silane is not eliminated from **3b** under thermal conditions; dihydrogen elimination occurs instead, again in contrast to predictions by the theory of 3c–2e σ-complexes. Another consequence of IHI is the remarkable thermal stability of **4** and **8** and their inertness towards halogenated solvents.

The main structural trends as well as the occurrence of an Nb–H →Si–Cl* electron density transfer were confirmed by DFT calculations. The presence of direct Si–H bonding contacts also follows from high Wiberg bond indices and observable bond paths found in the electron density Laplacian analysis of complex **3b** and its model **11**, and is supported by the NBO analysis. The calculation results demonstrate that the interligand interactions in the chlorosilyl complexes are stronger than those in the SiH_3 complexes. This fact is in clear contradiction of the σ-complex description of the interligand interactions in these compounds, since the latter theory predicts stronger H–Si bonding in complexes with more electropositive groups on silicon. Also, in the σ-bond complexes stronger H–Si bonding is accompanied by weaker M–Si bonds, in sharp contrast with our experimental observations and the calculation results. Our results by no means disprove the validity of the σ-complex description for certain classes of compounds, however. The principal conclusion of our studies is that strong experimental and theoretical evidence exists that electron-rich silyl hydride complexes exhibit a different type of interligand interaction, better described by the IHI theory.

Reactivity studies presented here suggest that not only is IHI a solid-state phenomenon, but it also accounts for a remarkable stabilization of some niobocene silyl hydrides in solution. Our NMR relaxation experiments revealed good correspondence between the structures observed in solution and the solid-state structures and also good correspondence with the calculation results for model compounds.[45] However, we were unable to establish a correlation between the structural (bond lengths) and NMR (coupling constants) parameters for our niobocene silyl hydrides because of the unfavourable influence of the quadrupolar niobium nucleus. Discovery of such a correlation is an important goal and will apparently require the study of other metal systems. Another task is to find out how variation of the metal and ligand influences the strength of interligand silyl–hydride interac-

0947-6539/99/0510-2960 $ 17.50+.50/0 *Chem. Eur. J.* **1999**, *5*, No. 10

tions. These studies are currently under way and our preliminary results are in accord with the IHI description.[46] Also, since the proposed hypervalent interligand interaction in transition metal silyl hydrides can be relevant to the initial stages of hydrogen migration onto the silyl ligands, the realization of complete migration is highly desirable.

Experimental Section

General methods: All manipulations were carried out using conventional Schlenk techniques. Solvents were dried over sodium or sodium benzophenone ketyl and distilled into the reaction vessel by high-vacuum gas-phase transfer. NMR spectra were recorded on a Varian VXR-400 spectrometer (^{1}H, 400 MHz; ^{13}C, 100.4 MHz, ^{29}Si, 23.9 MHz, ^{19}F, 376.3 MHz). IR spectra were obtained in Nujol with an FTIR Perkin-Elmer series 1600 spectrometer. $HSiMe_2Cl$ and $HSi(OEt)_3$ were purchased from Merck and $HSiMe_2Ph$ was from Aldrich. $[Cp_2NbBH_4]$[47] and $[Cp_2NbH_3]$[48] were prepared according to literature methods.

$[Cp_2NbH_2(Si(OEt)_3)]$ (1): To a solution of $[Cp_2NbBH_4]$ (0.428 g, 1.8 mmol) and $HSi(OEt)_3$ (2.0 mmol) in toluene (20 mL) was added a small excess of NEt_3 (0.15 mL, 2 mmol). The solution immediately turned brown. The mixture was stirred for 1 h. All volatiles were removed in vacuo and the residue was recrystallized from diethyl ether to give a yellow compound. Yield: 0.714 g (2.24 mmol, 82%). ^{1}H NMR ([D$_6$]benzene): $\delta = 4.75$ (s, 10H; Cp), 4.07 (q, ^3J(H, H) = 6.8 Hz, 6H; CH_2); 1.47(t, ^3J(H, H) = 6.8 Hz, 9H; CH_3), −5.12 (s, 2H; Nb–H); ^{13}C NMR ([D$_6$]benzene): $\delta = 88.19$ (Cp), 57.79 (CH_2), 18.34 (CH_3); $C_{16}H_{27}NbO_3Si$ (388.37): calcd. C 49.48, H 7.01; found C 49.10, H 7.15.

$[Cp_2NbH_2(SiPhMe_2)]$ (2): Compound **2** was prepared analogously to **1**. The product was recrystallized from hexane. Yield: 75%. ^{1}H NMR ([D$_6$]benzene): $\delta = 7.10$–7.70 (m, 5H; Ph), 4.57 (s, 10H; Cp), 0.74 (s, 6H; CH_3), −4.72 (s, 2H; Nb–H); ^{13}C NMR ([D$_6$]benzene): 126.7, 127.4, 128.2, 133.6, 134.3 (Ph), 87.9(Cp), 11.4 (CH_3). Other characterization data were as reported in the literature.

$[Cp_2NbH_2(SiMe_2Cl)]$ (3a and 3b)

Method a: $[Cp_2NbH_3]$ (0.728 g, 3.22 mmol) in toluene (20 mL) was treated with $HSiMe_2Cl$ (1.5 mL, 16.1 mmol). The mixture was heated for 4 h at 50–60 °C. All volatiles were removed in vacuo from the resultant yellow solution to give a light beige powder. Yield: 0.714 g (2.24 mmol, 70%).

Method b: The method was analogous to the preparation of **1**. The product was recrystallized from hexane. Yield: 78%. IR (Nujol): $\tilde{\nu}_{Nb-H} = 1693.9$ cm^{-1} with a shoulder on the left.

3b: ^{1}H NMR ([D$_6$]benzene): $\delta = 4.69$ (s, 10H; Cp), 0.80 (s, 6H; CH_3), −4.42 (s, 1H; Nb–H), −4.61 (s, 1H; Nb–H); ^{13}C NMR ([D$_6$]benzene): $\delta = 89.22$ (Cp), 13.28 (CH_3); ^{29}Si NMR ([D$_6$]benzene): $\delta = 88.7$ (s).

3a: ^{1}H NMR ([D$_6$]benzene): $\delta = 4.61$ (s, 10H; Cp), 0.91 (s, 6H; CH_3), −4.80 (s, 2H; Nb–H); ^{13}C NMR ([D$_6$]benzene): $\delta = 88.53$ (Cp), 17.51 (CH_3); ^{29}Si NMR ([D$_6$]benzene): $\delta = 83.9$ (s). $C_{12}H_{18}ClNbSi$ (318.71): calcd. C 45.22, H 5.69; found C 43.85, H 5.79.

$[Cp_2NbH(SiMe_2Cl)_2]$ (4)

Method a: $[Cp_2NbH_3]$ (1.93 g, 8.53 mmol) in toluene (30 mL) was treated with $HSiMe_2Cl$ (4.0 mL, 36 mmol). The mixture was heated for 4 h at 95 °C. All volatiles were removed in vacuo and the residue was recrystallized from diethyl ether. Yield of light beige powder: 2.96 g (7.20 mmol, 84%).

Method b: $[Cp_2Nb(C_2H_3Ph)H]$ (0.417 g, 1.27 mmol) was treated with $HSiClMe_2$ (0.70 mL, 6.35 mmol) in toluene (8 mL). The mixture was heated at 70 °C for 2 h, affording a brown solution. The solvent was removed in vacuo and the residue extracted with 150 mL of pentane. Recrystallization from Et_2O gave **3** as large, well-shaped pale crystals. Yield: 0.320 g (0.78 mmol, 61%). IR (Nujol): $\tilde{\nu}_{Nb-H} = 1722.4$ cm^{-1}. ^{1}H NMR ([D$_8$]toluene): $\delta = 4.65$ (s, 10H; Cp), 0.61 (s, 6H; Me), −5.15 (br s, 1H; H); ^{13}C NMR ([D$_8$]toluene): $\delta = 92.46$ (s; Cp), 13.56 (s; Me); ^{29}Si {^{1}H} NMR ([D$_8$]toluene): $\delta = 90.0$ (s); ^{1}H NMR ([D$_6$]benzene): $\delta = 4.65$ (s, 10H; Cp), 0.61 (s, 6H; CH_3), −5.18 (s, 1H; Nb–H); ^{1}H NMR ($CDCl_3$): $\delta = 5.32$ (s, 10H; Cp), 0.92 (s, 6H; CH_3), −4.93 (s, 1H; Nb–H); $C_{14}H_{23}Cl_2NbSi_2$ (411.31): calcd. C 40.88, H 5.64; found C 40.52, H 5.49.

$[Cp_2Nb(SiPhMe_2)_2H]$ (6): $[Cp_2Nb(C_2H_3Ph)H]$ (0.437 g, 1.33 mmol) was treated with $HSiPhMe_2$ (0.63 mL, 4.00 mmol) in toluene (8 mL). The mixture was heated at 70 °C for 3 h, affording a brown solution. The solvent was removed in vacuo and the residue extracted with pentane (150 mL). Recrystallization from Et_2O gave **6** in the form of large, light yellow crystals. Yield: 0.270 g (0.55 mmol, 41%). ^{1}H NMR ([D$_6$]benzene): $\delta = 4.33$ (s, 10H; Cp), 0.60 (s, 6H; Me), −3.23 (br s, 1H; H); ^{13}C NMR ([D$_6$]benzene): $\delta = 150.60$, 134.20, 127.88, 127.59 (s; Ph), 89.78 (s; Cp), 7.84 (s, Me); $C_{26}H_{33}NbSi_2$ (494.61): calcd. C 63.13, H 6.72; found C 62.87, H 6.55.

$[Cp_2NbH(SiHMe_2)_2]$ (7): $LiAlH_4$ (0.5 g) was added to **4** (0.988 g, 2.55 mmol) in diethyl ether (20 mL) with rapid stirring. The mixture was left overnight. The solution was filtered and the residue was washed with diethyl ether (10 mL). Water was added slowly at 0 °C to the combined diethyl ether fractions. The resultant yellow solution was decanted from the red oil and dried in vacuo. The yellow product was recrystallized from hexane. Yield: 0.672 g (1.96 mmol, 77%). IR (Nujol): $\tilde{\nu}_{Si-H} = 1987.6$ cm^{-1}, $\tilde{\nu}_{Nb-H} = 1737.1$ cm^{-1}; ^{1}H NMR ([D$_6$]benzene): $\delta = 4.98$ (h, ^3J(H, H) = 3.5 Hz, 2H; Si–H), 4.36 (s, 10H; Cp), 0.49 (s, ^3J(H, H) = 3.5 Hz, 6H; Me), −3.82 (b s, 1H; H); ^{13}C NMR ([D$_6$]benzene): $\delta = 89.47$ (s; Cp), 5.28 (s; Me); $C_{14}H_{25}NbSi_2$ (342.42): calcd. C 49.11; H 7.36; found C 48.81, H 7.13.

$[Cp_2NbH(SiFMe_2)_2]$ (8): $[Ph_3C][PF_6]$ (0.484 g, 2.50 mmol) in THF (30 mL) was added to $[Cp_2NbH(SiMe_2H)_2]$ (0.427 g, 1.25 mmol) in THF (4 mL) with rapid stirring. The mixture was then stirred for 20 min. The solution was filtered and dried in vacuo to give a brown oil, which was extracted with toluene (2 × 15 mL) and dried in vacuo. The residue was dissolved in pentane (20 mL) and left overnight at −26 °C. The cold solution was decanted from the resultant pale crystals. Yield: 0.179 g (0.53 mmol, 42%). IR (Nujol): $\tilde{\nu}_{Nb-H} = 1722.7$ cm^{-1}; ^{1}H NMR ([D$_6$]benzene): $\delta = 4.53$ (s, 10H; Cp), 0.52 (d, ^3J(H, H) = 7.5 Hz, 12H; Me), −5.26 (br s, 1H; H); ^{13}C NMR ([D$_6$]benzene): $\delta = 88.8$ (s; Cp), 10.88 (s, ^2J(H, H) = 14.1 Hz; Me); ^{19}F NMR ([D$_6$]benzene): $\delta = -125.6$. (s); $C_{14}H_{23}F_2NbSi_2$ (378.41): calcd. C 44.44, H 6.13; found C 44.68, H 6.37.

$[Cp_2NbH(SiMe_2Br)_2]$ (9): $[Cp_2NbH(SiMe_2H)_2]$ (0.655 g, 1.91 mmol) in diethyl ether (30 mL) was treated with Br_2·dioxane complex (0.835 g, 3.37 mmol). An immediate reaction occurred to give a beige precipitate and a yellow solution. The solution was filtered and the precipitate was washed with diethyl ether. Yield of the precipitate: 0.458 g. Solvent removal from the combined fractions gave large, pale crystals of **9**. Yield: 0.240 g (0.480 mmol, 25%). IR (Nujol): $\tilde{\nu}_{Nb-H} = 1717$ cm^{-1}; ^{1}H NMR ([D$_6$]benzene): $\delta = 4.70$ (s, 10H; Cp), 0.71 (s, 6H; Me), −5.16 (b s, 1H; H); ^{13}C NMR ([D$_6$]benzene): $\delta = 93.76$ (s; Cp), 14.08 (s; Me); $C_{14}H_{23}Br_2NbSi_2$ (500.23): calcd. C 33.62, H 4.63; found C 34.18, H 4.36.

Crystal structure determinations

3b: The pale crystals of **3b** were grown from a solution of the compound in diethyl ether. A crystal (0.46 mm × 0.26 mm × 0.28 mm) was covered with oil and mounted at 193(2) K on an Enraf-Nonius CAD-4 diffractometer. Crystal data: $M_r = 318.71$; orthorhombic, space group *Pnma*, $a = 11.747(6)$, $b = 13.222(9)$, $c = 8.425(3)$ Å, $Z = 4$, $V = 1844.9(6)$ Å^3, $\rho_{calcd} = 1.618$ g cm^{-3}. Data collection: ϑ range from 2.87 to 27.97°, hkl range −2 to 15, −17 to 8, −11 to 0, 2116 measured reflections, 1390 unique [R(int) = 0.1130], analytical absorption correction based on ψ scans ($\mu = 1.182$ mm^{-1}, $T_{max} = 0.987$, $T_{main} = 0.760$). The unit cell parameters were determined using 25 accurately centred reflections; two reflections were measured every 2 h for orientation and decay control. The structure amplitudes for independent reflections were obtained after the usual Lorentz and polarization corrections. The structure was solved by direct methods[49] and refined by full-matrix least-squares procedures[50] against F^2. Only the reflections with $F_o^2 > 2\sigma F_o^2$ were used in the refinements. Hydrogen atoms were found from the difference map and were refined isotropically. In the final cycles of refinement, all the non-hydrogen atoms were refined with anisotropic temperature parameters. $R1 = 0.0437$ and $wR2 = 0.1157$ (only observed reflections), and $R1 = 0.0490$ and $wR2 = 0.1186$ (all data), 78 parameters, GOOF = 1.060. The largest peak in the final difference Fourier map had an electron density of 0.444 e Å^{-3} and the lowest hole one of −0.485 e Å^{-3}.The location and magnitude of the residual electron density were of no chemical significance.

4: The yellow crystals of **4** were grown from a solution of the compound in diethyl ether. A crystal (0.36 mm × 0.23 mm × 0.16 mm) was covered with oil and mounted at 190(2) K on an Enraf-Nonius CAD-4 diffractometer. Crystal data: $M_r = 494.61$; orthorhombic, space group *Pbcn*, $a = 15.356(3)$,

$b = 8.856$ (2), $c = 17.522(4)$ Å, $Z = 4$, $V = 2382.9(8)$ Å^3, $\rho_{calcd} = 1.379$ g cm^{-3}. Data collection: ϑ range from 2.32 to 26.94°, hkl range -22 to 0, -10 to 0, 0 to 19, 1539 measured reflections, 1539 unique [R(int) = 0.000], analytical absorption correction based on ψ scans ($\mu = 0.616$ mm^{-1}, $T_{max} = 0.834$, $T_{main} = 0.746$). The unit cell parameters were determined using 25 accurately centred reflections; two reflections were measured every 2 h for orientation and decay control. The structure amplitudes for independent reflections were obtained after the usual Lorentz and polarization corrections. The structure was solved by direct methods[49] and refined by full-matrix least-squares procedures[50] against F^2. Only the reflections with $F_o^2 > 2\sigma F_o^2$ (1532) were used in the refinements. Hydrogen atoms were found from the difference map and were refined isotropically. In the final cycles of refinement, all the non-hydrogen atoms were refined with anisotropic temperature parameters. $R1 = 0.0312$ and $wR2 = 0.0815$ (only observed reflections), and $R1 = 0.0321$ and $wR2 = 0.0826$ (all data), 199 parameters, GOOF = 1.044. The largest peak in the final difference Fourier map had an electron density of 1.38 e Å^{-3} and the lowest hole one of -0.440 e Å^{-3}.The location and magnitude of the residual electron density were of no chemical significance.

6: The pale beige crystals of **6** were grown from a solution of the compound in diethyl ether. A crystal (0.52 mm × 0.44 mm × 0.26 mm) was covered with oil and mounted at 173(2) K on an Enraf-Nonius CAD-4 diffractometer. Crystal data: $M_r = 411.31$; orthorhombic, space group $Pnma$, $a = 16.584(3)$, $b = 13.214(2)$, $c = 8.419(2)$ Å, $Z = 4$, $V = 1844.9(6)$ Å^3, $\rho_{calcd} = 1.481$ g cm^{-3}. Data collection: ϑ range from 2.46 to 29.96°, hkl range 0 to 23, 0 to 18, 0 to 9, 2674 measured reflections, 2221 unique [R(int) = 0.0237], analytical absorption correction based on ψ scans ($\mu = 1.05$ mm^{-1}, $T_{max} = 0.937$, $T_{main} = 0.843$). The unit cell parameters were determined using 25 accurately centred reflections; two reflections were measured every 2 h for orientation and decay control. The structure amplitudes for independent reflections were obtained after the usual Lorentz and polarization corrections. The structure was solved by direct methods[49] and refined by full-matrix least-squares procedures[50] against F^2. Only the reflections with $F_o^2 > 2\sigma F_o^2$ (2214) were used in the refinements. Hydrogen atoms were found from the difference map and were refined isotropically. In the final cycles of refinement, all the non-hydrogen atoms were refined with anisotropic temperature parameters. $R1 = 0.0345$ and $wR2 = 0.1027$ (only observed reflections), and $R1 = 0.0367$ and $wR2 = 0.1151$ (all data), 95 parameters, GOOF = 1.240. The largest peak in the final difference Fourier map had an electron density of 1.028 e Å^{-3} and the lowest hole one of -2.04 e Å^{-3}.The location and magnitude of the residual electron density were of no chemical significance.

8: The pale yellow crystals of **8** were grown from a solution of the compound in hexane. A crystal (0.24 mm × 0.08 mm × 0.06 mm) was covered with oil and mounted at 150(2) K on a Siemens three-circle diffractometer with area CCD detector (SMART system). Crystal data: $M_r = 411.31$; orthorhombic, space group $P2_12_12_1$, $a = 7.9740(1)$, $b = 8.7739(2)$, $c = 23.1718(4)$ Å, $Z = 4$, $V = 1621.17(6)$ Å^3, $\rho_{calcd} = 1.624$ g cm^{-3}. Data collection: ϑ range from 1.746 to 27.51°, hkl range -10 to 10, -11 to 11, -21 to 30, 11772 measured reflections, 3716 unique [R(int) = 0.0687], analytical absorption correction based on ψ scans ($\mu = 0.90$ mm^{-1}, $T_{max} = 1.00$, $T_{main} = 0.862$). The structure amplitudes for independent reflections were obtained after the usual Lorentz and polarization corrections. The structure was solved by direct methods[49] and refined by full-matrix least-squares procedures[50] against F^2. Only the reflections with $F_o^2 > 2\sigma F_o^2$ (3578) were used in the refinements. Hydrogen atoms were found from the difference map and were refined isotropically. In the final cycles of refinement, all the non-hydrogen atoms were refined with anisotropic temperature parameters. $R1 = 0.0392$ and $wR2 = 0.0730$ (only observed reflections), and $R1 = 0.0540$ and $wR2 = 0.0820$ (all data), 265 parameters, GOOF = 1.069. The largest peak in the final difference Fourier map had an electron density of 0.444 e Å^{-3} and the lowest hole one of -0.485 e Å^{-3}.The location and magnitude of the residual electron density were of no chemical significance. The absolute structure parameter was 0.00(5).

9: The pale yellow crystals of **9** were grown from a solution of the compound in diethyl ether. A crystal (0.06 mm × 0.12 mm × 0.42 mm) was covered with oil and mounted at 293(2) K on an Enraf-Nonius CAD-4 diffractometer. Crystal data: $M_r = 500.23$; orthorhombic, space group $Pnma$, $a = 16.746(6)$, $b = 13.349(5)$, $c = 8.607(3)$ Å, $Z = 4$, $V = 1924.0(12)$ Å^3, $\rho_{calcd} = 1.727$ g cm^{-3}. Data collection: ϑ range from 2.43 to 24.98°, hkl range -19 to 3, -4 to 15, -9 to 10, 2404 measured reflections, 1619 unique [R(int) = 0.0725], analytical absorption correction based on ψ-scans ($\mu = 4.891$ mm^{-1}, $T_{max} = 0.936$, $T_{main} = 0.765$). The unit cell parameters were determined using 25 accurately centred reflections; two reflections were measured every 2 h for orientation and decay control. The structure amplitudes for independent reflections were obtained after the usual Lorentz and polarization corrections. The structure was solved by direct methods[49] and refined by full-matrix least-squares procedures[50] against F^2. Only the reflections with $F_o^2 > 2\sigma F_o^2$ (1604) were used in the refinements. Hydrogen atoms were found from the difference map and were refined isotropically. In the final cycles of refinement, all the non-hydrogen atoms were refined with anisotropic temperature parameters. $R1 = 0.0351$ and $wR2 = 0.0769$ (only observed reflections), and $R1 = 0.0630$ and $wR2 = 0.0853$ (all data), 141 parameters, GOOF = 0.999. The largest peak in the final difference Fourier map had an electron density of 0.655 e Å^{-3} and the lowest hole one of -0.612 e Å^{-3}.The location and magnitude of the residual electron density were of no chemical significance.

Crystallographic data (excluding structure factors) for the structures reported in this paper have been deposited with the Cambridge Crystallographic Data Centre as supplementary publication nos. CCDC-105586 (**3b**), CCDC-105588 (**4**), CCDC-105589 (**6**), CCDC-105590 (**8**) and CCDC-105591 (**9**). Copies of the data can be obtained free of charge on application to CCDC, 12 Union Road, Cambridge CB2 1EZ, UK (fax: (+44) 1223-336-033; e-mail: deposit@ccdc.cam.ac.uk).

Computational details: All calculations were carried out with the Gaussian 94 program package[51] using the density functional theory applying Becke's 1988 non-local exchange functional[52] in conjunction with Perdew's correlation functional,[53] commonly aliased as BP86. The valence double-ζ basis sets with the (341/321/31) contraction scheme for niobium, (31/31) for silicon and chlorine, and 6-31G*[54] for carbon and hydrogen were employed. The Si and Cl basis sets were additionally augmented by a polarization d function. To describe correctly the presumably weak Si–H interaction, the hydrides H were supplemented by a polarization p function. For Si and Cl, the "Stuttgart" quasi-relativistic effective core potentials (ECPs) [55] were used, while for Nb the quasi-relativistic "Los Alamos" ECP [56] was employed. The natural bond orbital analysis[36] was performed with the BP86 optimized structures using the Gaussian NBO 3.1 program incorporated into Gaussian 94. For this purpose, the Kohn–Sham orbitals resulting from the DFT calculations were employed. The topological analysis of electron density,[37] also known as the atoms-in-molecules theory, was applied to corresponding electron densities. Since the deficiency of electron density in areas close to the nuclei of Nb, Si and Cl atoms at which ECPs are applied may cause improper results, such as spurious density maxima and critical points, the respective single-atom core densities were added as described in reference [57]. For the topological analysis, the EXTREME program was employed.[58]

Acknowledgement

The Russian Foundation for Basic Research is acknowledged for financial support of this work. We thank the Royal Society for an award to L.G.K.

[1] J. P. Collman, L. S. Hegedus, J. R. Norton, R. G. Finke, *Principles and Application of Organotransition Metal Chemistry*, 2nd ed., University Science Books, Mill Valley, California, **1987**.

[2] For reviews see: a) G. J. Kubas, *Acc. Chem. Res.* **1988**, *21*, 120; b) U. Schubert *Adv. Organomet. Chem.* **1990**, *30*, 151; c) R. H. Crabtree, *Acc. Chem. Res.* **1990**, *23*, 95; d) P. G. Jessop, R. H. Morris, *Coord. Chem. Rev.* **1992**, *121*, 155; e) R. H. Crabtree, *Angew. Chem.* **1993**, *105*, 828; *Angew. Chem. Int. Ed. Engl.* **1993**, *32*, 789.

[3] a) G. I. Nikonov, L. G. Kuzmina, D. A. Lemenovskii, V. V. Kotov, *J. Am. Chem. Soc.* **1995**, *117*, 10133; b) G. I. Nikonov, L. G. Kuzmina, D. A. Lemenovskii, V. V. Kotov, *J. Am. Chem. Soc.* **1996**, *118*, 6333 (correction).

[4] T. I. Gountchev, T. D. Tilley, *J. Am. Chem. Soc.* **1997**, *119*, 12831.

[5] a) D. H. Berry, Q. Jiang, *J. Am. Chem. Soc.* **1987**, *109*, 6210; b) D. H. Berry, T. S. Koloski, P. J. Carroll, *Organometallics* **1990**, *9*, 2952; c) Q.

  0947-6539/99/0510-2962 $ 17.50+.50/0

Jiang, P. J. Carroll, D. H. Berry, *Organometallics* **1991**, *10*, 3648; d) T. S. Koloski, D. C. Pestana, P. J. Carroll, D. H. Berry, *Organometallics* **1994**, *13*, 489.

[6] a) G. L. Casty, C. G. Lugmair, N. S. Radu, T. D. Tilley, J. F. Walzer, D. Zargarian, *Organometallics* **1997**, *16*, 8; b) S. Seebald, G. Kickelblick, F. Müller, U. Schubert, *Chem. Ber.* **1996**, *129*, 1131; c) Z. Xue, L. Li, L. K. Hoyt, J. B. Diminnie, J. Pollitte, *J. Am. Chem. Soc.* **1994**, *116*, 2169; d) U. Schubert, A. Schenkel, *Chem. Ber.* **1988**, *121*, 939; e) J. Arnold, T. D. Tilley, A. L. Rheingold, S. J. Geib, *Organometallics* **1987**, *6*, 473; f) T. D. Tilley, *Organometallics* **1985**, *4*, 1452; g) Ya. A. Ol'dekop, V. A. Knizhnikov, *Zh. Obshch. Khim.* **1981**, *51*, 723; h) L. G. Casty, T. D. Tilley, *Organometallics* **1997**, *16*, 4746.

[7] a) M. L. H. Green, A. K. Hughes, *J. Organomet. Chem.* **1996**, *506*, 221; b) V. K. Dioumaev, J. F. Harrod, *Organometallics* **1996**, *15*, 3859; c) A. Antiñolo, F. Carrillo, M. Fajardo, A. Otero, M. Lanfranchi, M. A. Pellinghelli, *Organometallics* **1995**, *14*, 1518; d) E. Spaltenstein, P. Palma, K. A. Kreutzer, C. A. Willoughby, W. M. Davis, S. L. Buchwald, *J. Am. Chem. Soc.* **1994**, *116*, 10308; e) K. A. Kreutzer, R. A. Fischer, W. M. Davis, E. Spaltenstein, S. L. Buchwald, *Organometallics* **1991**, *10*, 4031; f) T. Takahashi, M. Hasegawa, N. Suzuki, M. Saburi, C. J. Rousset, P. E. Fanwick, E. Negishi, *J. Am. Chem. Soc.* **1991**, *113*, 8564; g) M. D. Curtis, L. G. Bell, W. M. Butler, *Organometallics* **1985**, *4*, 701.

[8] a) T. D. Tilley, *Acc. Chem. Res.* **1993**, *26*, 22; b) H. G. Woo, W. Freeman, T. D. Tilley, *Organometallics* **1992**, *11*, 2198; c) H. G. Woo, T. D. Tilley, *J. Am. Chem. Soc.* **1989**, *111*, 8043.

[9] a) H. G. Woo, J. F. Harrod, J. Hénique, E. Samuel, *Organometallics* **1993**, *12*, 2883; b) J. Britten, Y. Mu, J. F. Harrod, J. Polowin, M. C. Baird, E. Samuel, *Organometallics* **1993**, *12*, 2672; c) E. Samuel, Y. Mu, J. F. Harrod, Y. Dromzee, Y. Jeannin, *J. Am. Chem. Soc.* **1990**, *112*, 3435; d) J. F. Harrod, T. Ziegler, V. Tschinke, *Organometallics* **1990**, *9*, 897; e) C. Aitken, J.-P. Barry, F. Gauvin, J. F. Harrod, A. Malek, D. Rousseau, *Organometallics* **1989**, *8*, 1732; f) C. Aitken, J. F. Harrod, E. Samuel, *J. Am. Chem. Soc.* **1986**, *108*, 4059; g) C. Aitken, J. F. Harrod, E. Samuel, *Can. J. Chem.* **1986**, *64*, 1677; h) L. Procopio, P. J. Carroll, D. H. Berry, *Polyhedron* **1995**, *14*, 45; i) Q. Jiang, D. C. Pestana, P. J. Carroll, D. H. Berry, *Organometallics* **1994**, *13*, 3679; j) D. H. Berry, Q. Jiang, *J. Am. Chem. Soc.* **1989**, *111*, 8049; k) D. H. Berry, Q. Jiang, *J. Am. Chem. Soc.* **1987**, *109*, 6210; l) D. H. Berry, Q. Jiang, *J. Am. Chem. Soc.* **1987**, *109*, 3777.

[10] F. N. Tebbe, G. W. Parshal, *J. Am. Chem. Soc.* **1971**, *93*, 3793.

[11] Yu. V. Skripkin, I. L. Eremenko, A. A. Pasynskii, Yu. T. Struchkov, V. E. Shklover, *J. Organomet. Chem.* **1984**, *267*, 285.

[12] B. J. Burger, B. D. Santarsiero, M. S. Trimmer, J. E. Bercaw, *J. Am. Chem. Soc.* **1988**, *110*, 3134.

[13] M. L. H. Green, A. K. Hughes, P. Mountford, *J. Chem. Soc. Dalton Trans.* **1991**, 1407.

[14] See, for example: a) D. H. Berry, J. H. Chey, H. S. Zipin, P. J. Carroll, *J. Am. Chem. Soc.* **1990**, *112*, 452; b) A. Antiñolo, M. Fajardo, C. Lopez Mardomingo, A. Otero, C. Sanz-Bernabé, *J. Organomet. Chem.* **1989**, *369*, 187.

[15] H. Kobayashi, K. Ueno, H. Ogino, *Organometallics* **1995**, *14*, 5490.

[16] R. R. Schrock, P. R. Sharp, *J. Am. Chem. Soc.* **1975**, *97*, 6577.

[17] J. A. Labinger, K. S. Wong, *J. Organomet. Chem.* **1979**, *170*, 373.

[18] H. A. Bent, *Chem. Rev.* **1961**, *61*, 275.

[19] For the structures of complexes with the fragment M–SiR–Cl (R = aryl, alkyl), see: a) K. E. Lee, A. M. Arif, J. A. Gladysz, *Chem. Ber.* **1991**, *124*, 309; b) B. R. Jagirdar, R. Palmer, K. J. Klabunde, L. Radonovich, *Inorg. Chem.* **1995**, *34*, 278; c) M. K. Hays, R. Eisenberg, *Inorg. Chem.* **1991**, *30*, 2623.

[20] E. A. Zarate, V. O. Kennedy, J. A. McCune, R. S. Simons, C. A. Tessier, *Organometallics* **1995**, *14*, 1802.

[21] a) U. Schubert, G. Kraft, E. Walther, *Z. Anorg. Allg. Chem.* **1984**, *519*, 96; b) U. Schubert, G. Scholz, J. Müller, K. Ackerman, B. Wörle, R. F. D. Stansfield, *J. Organomet. Chem.* **1986**, *306*, 303.

[22] A. A. Macharashvili, V. E. Shklover, Yu. T. Struchkov, G. I. Oleneva, E. P. Kramorova, A. G. Shipov, Yu. I. Baukov, *J. Chem. Soc. Chem. Commun.* **1988**, 683.

[23] R. Kergoat, M. M. Kubicki, J. E. Guerchais, N. C. Norman, A. G. Orpen, *J. Chem. Soc. Dalton Trans.* **1982**, 633.

[24] I. Bkouche-Waksman, C. Bois, J. Sala-Pala, J. E. Guerchais, *J. Organomet. Chem.* **1980**, *195*, 307.

[25] T. R. Ward, H.-B. Bürgi, F. Gilardoni, J. Weber, *J. Am. Chem. Soc.* **1997**, *119*, 11974.

[26] a) M. J. Michalczyk, M. J. Kink, K. J. Haller, R. West, J. Michl, *Organometallics* **1986**, *5*, 531; b) A. J. Millevolte, D. R. Powell, S. G. Johnson, R. West, *Organometallics* **1992**, *11*, 1091.

[27] R. S. Grev, H. F. Schaefer, *J. Am. Chem. Soc.* **1987**, *109*, 6577.

[28] It is essential to note that the shortest nonbonding contact between atoms X and Y can be even less than the longest bonding contact between the same atoms, since these contacts are usually observed for different ligand environments for X and Y. In other words, the criterion for the shortest nonbonding contact cannot serve as a criterion for the longest bonding contact.

[29] R. S. Simons, C. A. Tessier, *Organometallics* **1996**, *15*, 2604.

[30] One can argue that in the resulting distorted trigonal bipyramid, the X-Si-Nb angle should be close to 90° with the hybridization at silicon described as $sp^2 + p$. In fact the silicon s orbital has little propensity to mix with the p orbitals.[31] Thus "hybridization" at silicon can be better described as $s + p^3$, where $s + p^2$ is responsible for bonding with Me groups and Nb, and the third p orbital serves to bind Cl and H groups. Moreover, in the latter case the Si–Cl antibonding orbital is also oriented closer to the Nb–H bond, making the interaction stronger.

[31] See, for example: K. Kobayashi, S. Nagase, *Organometallics* **1997**, *16*, 2489.

[32] a) T. A. Albright, J. K. Burdett, M.-H. Whangbo, *Orbital Interactions in Chemistry*, Wiley, New York, **1985**; b) R. G. Pearson, *Orbital Topology and Elementary Processes*, Wiley, New York, **1976**, Chapter 1.

[33] See for example: a) M.-F. Fan, Z. Lin, *Organometallics* **1997**, *16*, 494; b) F. Maseras, A. Lledós, M. Costas, J. M. Poblet, *Organometallics* **1996**, *15*, 2947; c) J. Tomas, A. Lledós, Y. Jean, *Organometallics* **1998**, *17*, 190; d) R. Gelabert, M. Moreno, J. M. Lluch, A. Lledós, *J. Am. Chem. Soc.* **1997**, *119*, 9840.

[34] V. I. Bakhmutov, E. V. Vorontsov, G. I. Nikonov, D. A. Lemenovskii, *Inorg. Chem.* **1998**, *37*, 279.

[35] See, for example: a) K. Hübler, P. A. Hunt, S. M. Maddlock, C. E. F. Rickard, W. R. Roper, D. M. Salter, P. Schwerdtfeger, L. J. Wright, *Organometallics* **1997**, *16*, 5076; b) M.-F. Fan, Z. Lin, *J. Am. Chem. Soc.* **1996**, *118*, 9915; c) ref. [32a].

[36] a) J. P. Foster, F. Weinhold, *J. Am. Chem. Soc.*, **1980**, *102*, 7211; b) A. E. Reed, F. Weinhold, *J. Chem. Phys.* **1983**, *78*, 4066; c) A. E. Reed, L. A. Curtiss, F. Weinhold, *Chem. Rev.* **1988**, *88*, 899.

[37] R. F. Bader, *Atoms in Molecules: A Quantum Theory*, Clarendon, New York, **1990**.

[38] K. Hübler, U. Hübler, W. Roper, P. Schwerdtfeger, L. J. Wright, *Chem. Eur. J.* **1997**, *3*, 1608.

[39] J. Cioslowski, S. T. Mixon, *J. Am. Chem. Soc.* **1992**, *114*, 4382.

[40] a) R. F. W. Bader, P. J. MacDougall, C. D. H. Lau, *J. Am. Chem. Soc.* **1984**, *106*, 1594; b) R. F. W. Bader, H. Essén, *J. Chem. Phys.* **1984**, *80*, 1943.

[41] a) D. Cremer, E. Kraka *Angew. Chem.* **1984**, *96*, 612; *Angew. Chem. Int. Ed. Engl.* **1984**, *23*, 627; b) D. Cremer, E. Kraka, *Croat. Chem. Acta* **1984**, *57*, 1259.

[42] S. Camanyes, F. Maseras, M. Moreno, A. Lledós, J. M. Lluch, J. Bertrán, *J. Am. Chem. Soc.* **1996**, *118*, 4617.

[43] An analogous "parallel" approach of a C–H bond to a metal has been previously addressed theoretically in: a) H. H. Brintzinger, *J. Organomet. Chem.* **1979**, *171*, 337; b) J.-Y. Saillard, R. Hoffmann, *J. Am. Chem. Soc.* **1984**, *106*, 2006.

[44] M.-F. Fan, Z. Lin, *Organometallics* **1998**, *18*, 1092.

[45] V. I. Bakhmutov, E. V. Vorontsov, J. A. K. Howard, D. A. Keen , L. G. Kuzmina, M. A. Leech, G. I. Nikonov, C. Wilson, *Inorg. Chem,* submitted.

[46] G. I. Nikonov, S. B. Duckett, L. G. Kuzmina, unpublished results.

[47] C. R. Lucas, M. L. H. Green, *Chem. Commun.* **1972**, 2005.

[48] G. I. Nikonov, D. A. Lemenovskii, J. Lorberth, *Organometallics* **1994**, *13*, 3127.

[49] G. M. Sheldrick, SHELXS-86 Program for Crystal Structure Solution, *Acta Crystallogr. Sect. C* **1990**, *146*, 467.

[50] G. M. Sheldrick, SHELXTL-96, Program for Crystal Structure Refinement, Universität Göttingen.

[51] Gaussian 94, Revision C.2, M. J. Frisch, G. W. Trucks, H. B. Schlegel, P. M. W. Gill, B. G. Johnson, M. A. Robb, J. R. Cheeseman, T. Keith,

G. A. Petersson, J. A. Montgomery, K. Raghavachari, M. A. Al-Laham, V. G. Zakrzewski, J. V. Ortiz, J. B. Foresman, J. Cioslowski, B. B. Stefanov, A. Nanayakkara, M. Challacombe, C. Y. Peng, P. Y. Ayala, W. Chen, M. W. Wong, J. L. Andres, E. S. Replogle, R. Gomperts, R. L. Martin, D. J. Fox, J. S. Binkley, D. J. Defrees, J. Baker, J. J. P. Stewart, M. Head-Gordon, C. Gonzalez, J. A. Pople, Gaussian, Inc., Pittsburgh, PA, **1995**.
[52] A. D. Becke, *Phys. Rev.* **1988**, *A38*, 3098.
[53] B. P. Perdew, *Phys. Rev.* **1986**, *B33*, 8822.
[54] R. Ditchfield, W. J. Hehre, J. A. Pople, *J. Chem. Phys.* **1971**, *54*, 724.
[55] A. Bergner, M. Dolg, W. Küchle, H. Stoll, H. Preuss, *Mol. Phys.* **1993**, *80*, 1431.
[56] P. J. Hay, W. R. Wadt, *J. Chem. Phys.* **1985**, *82*, 270.
[57] a) S. F. Vyboishchikov, A. Sierraalta, G. Frenking, *J. Comput. Chem.* **1997**, *3*, 416; b) J. Cioslowski, P. Piskorz, *Chem. Phys. Lett.* **1996**, *255*, 315.
[58] F. W. Biegler-König, EXTREME, McMaster University, Hamilton (ON), **1982**.

Received: November 16, 1998 [F1445]

  0947-6539/99/0510-2964 $ 17.50+.50/0